ISTANBUL TECHNICAL UNIVERSITY ★ GRADUATE SCHOOL

THE INVESTIGATION OF THERMO-RESPONSIVE POLYMERS EXHIBITING LCST WITH INTERACTIONS BETWEEN WATER MOLECULES BY QUANTUM MECHANICAL METHODS

M.Sc. THESIS

Fatma CAN KÜTÜK

Department of Polymer Science and Technology

Polymer Science and Technology Programme

JANUARY 2023

ISTANBUL TECHNICAL UNIVERSITY ★ GRADUATE SCHOOL

THE INVESTIGATION OF THERMO-RESPONSIVE POLYMERS EXHIBITING LCST WITH INTERACTIONS BETWEEN WATER MOLECULES BY QUANTUM MECHANICAL METHODS

M.Sc. THESIS

Fatma CAN KÜTÜK
(515181025)

Department of Polymer Science and Technology

Polymer Science and Technology Programme

Thesis Advisor: Prof. Dr. Nurcan TÜZÜN
Thesis Co-Advisor: Asst. Prof. Berkay SÜTAY

JANUARY 2023

ISTANBUL TEKNİK ÜNİVERSİTESİ ★ LİSANSÜSTÜ EĞİTİM ENSTİTÜSÜ

LCST DAVRANIŞI GÖSTEREN ISIYA DUYARLI POLİMERLERİN SU İLE ETKİLEŞİMLERİNİN KUANTUM MEKANIK YÖNTEMLERLE İNCELENMESİ

YÜKSEK LİSANS TEZİ

Fatma CAN KÜTÜK
(515181025)

Polymer Bilim ve Teknolojileri Anabilim Dalı

Polymer Bilim ve Teknolojisi Programı

Tez Danışmanı: Prof. Dr. Nurcan TÜZÜN
Eş Danışman: Dr. Öğr.Üyesi Berkay SÜTAY

OCAK 2023

Fatma CAN KÜTÜK, a M.Sc. student of ITU Graduate School student ID 515181025, successfully defended the thesis entitled "INVESTIGATION OF THERMO-RESPONSIVE POLYMERS EXHIBITING LCST WITH WATER MOLECULES INTERACTIONS BY QUANTUM MECHANICALS METHODS", which she prepared after fulfilling the requirements specified in the associated legislations, before the jury whose signatures are below.

Thesis Advisor :	**Prof. Dr. Nurcan TÜZÜN** Istanbul Technical University	.....
Co-advisor :	**Asst. Prof. Berkay SÜTAY** Istanbul Technical University	.....
Jury Members :	**Prof. Dr. Viktorya AVIYENTE** Bogazici University	.....
	Assoc. Prof. Dr. Bünyamin KARAGÖZ Istanbul Technical University	.....
	Asst. Prof. Yusuf Serhat İŞ Istanbul Gedik University	.....

Date of Submission : 30 December 2022
Date of Defense : 12 January 2023

To my family,

FOREWORD

In this part, I would like to express my sincere gratitude to all people who contributed to the completion of this thesis.

First place, I wish to express my gratitude and thankfulness to my advisors, Prof.Dr. Nurcan TÜZÜN and Asst.Prof. Berkay SÜTAY for their invaluable advice, continuous professional, emotional support and patience throughout my M.Sc. study. I am grateful to them for accepting me as my advisor and working with them has always been a pleasure.

I am eternally thankful for the support of my family that made me here today.

Finally, I would like to thank my dear husband, Enes KÜTÜK, whose faith in me has given me the courage and confidence to pursue my dreams.

January 2023

Fatma CAN KÜTÜK
(Chemist)

TABLE OF CONTENTS

Page

ABBREVIATIONS

LCST **:** Lower Critical Solution Temperature

UCST : Upper Critical Solutıon Temperature

B3LYP : Becke Style Three Parameter Functional in Combination with the Lee-Yang Parr Correlation Functional

DFT **:** Density Functional Theory

VPT : Volume Phase Transition

FH **:** Flory Huggins Theory

STO **:** Slater Type Orbitals

GTOs **:** Gaussian Type Orbitals

∆Gm **:** Gibbs Free Energy of Mixing

BSSE **:** Basis Set Superposition Error

CP **:** Counter Poise

ZPVE **:** Zero Point Vibrational Energy

SYMBOLS

Ψ	**:** Wavefunction
Å	**:** Angstrom
$\mathbf{r_{int}}$	**:** Intermolecular Distance
Φ	**:** Volume Fraction
χ	**:** Interaction Parameter
δ	**:** Hildebrand solubility parameters
$\mathbf{V_0}$	: Molar Volume
ΔS	: Entropy Change
b	: Kuhn Length
R	: End-to-end Distance
$\mathbf{T_\theta}$	**:** Theta Temperature
$\mathbf{E_{int}}$	**:** Interaction Energy

LIST OF TABLES

Page

LIST OF FIGURES

Page

THE INVESTIGATION OF THERMO-RESPONSIVE POLYMERS EXHIBITING LCST WITH INTERACTIONS BETWEEN WATER MOLECULES BY QUANTUM MECHANICAL METHODS

SUMMARY

Thermo-responsive polymers exhibiting the coil-to-globule phase transition at the lower critical solution temperature (LCST) have been the subject of great interest in the development of smart materials. As a result of LCST behavior in aqueous solutions, the polymers undergo a phase separation in water upon heating, resulting in a decreased solubility and a change in conformation from hydrated coil to collapsed globular for diluted solutions.

In this work, thermo-responsive polymers in aqueous solutions have been studied in terms of their conformational changes which plays a crucial role in determining the role of functional groups and their interactions with water. Poly (N-isopropylacrylamide) (PNIPAAm), Poly(N-vinylisobutyramide)(PNVIBA), and Poly(2-ethoxyethyl vinyl ether)(PEOVE) exhibiting LCST behavior in water were studied in order to examine structural changes by using Density Functional Theory (DFT). Geometry optimizations were carried out using the B3LYP functional and 6-31G(d,p) basis set, which are known to perform well in the geometry optimizations of organic molecules. The hydrogen bond interaction of the water molecule with the pentamer of these monomers, which is the longest oligomer chain optimized starting from the dimer molecules, was modeled by testing various configurations. Interaction energies were calculated by using different functionals such as B3LYP, LC-wPBE and CAM-B3LYP and 6-311G(2df,2pd) basis set for a quantitative interpretation of the hydrogen bond. The basis set superposition error (BSSE) was also considered in all interaction energy calculations. Interaction energies were also corrected by the addition of zero point energies (ΔZPE).

The effect of segment...solvent and segment...segment interactions on the conformation of the polymer chain were investigated in solvent media. The effect of the size of the oligomer on the conformation was also studied. In order to observe conformational changes in the backbones, Radius of gyration (Rg) and Root-mean-square deviation (RMSD) were calculated between the oligomer-water complexes and the unhydrated oligomer chain.

The calculations in this study aim to provide insight into the effect of intermolecular interactions on conformational transitions in single chains of thermo-responsive polymers. Based on our calculations, the increasing number of water molecules results in an increase in the strength of the interaction.

LCST DAVRANIŞI GÖSTEREN ISIYA DUYARLI POLİMERLERİN SU MOLEKÜLLERİ ARASINDAKİ ETKİLEŞİMLERİNİ KUANTUM MEKANİK YÖNTEMLERİYLE İNCELENMESİ

ÖZET

"Uyaranlara duyarlı polimerler" çevrelerindeki değişikliklere veya "uyaranlara" tepki olarak farklı kimyasal, fiziksel veya biyolojik davranışlar sergileyen polimerler olarak tanımlanmaktadır. Bir polimerin verdiği tepkiye göre uyaranlar fiziksel, kimyasal veya biyolojik uyaranlar olarak kategorize edilebilir. Polimerik malzemeler, seramik ve metallerden daha ucuz ve çalışması daha kolaydır, bu da onları "akıllı" malzemelerin ana grubunun bir parçası haline getirir. Polimerik "akıllı" malzemeler, fiziksel faktörlere (basınç, sıcaklık, ışık, ses, elektrik ve manyetik alanlar), kimyasal faktörlere (pH, çözücü bileşimi, iyonik mukavemet) ve biyolojik faktörlere (enzimler, reseptörler) maruz kaldıklarında fizikokimyasal özelliklerini önemli ölçüde değiştirebilirler.

Isıya-duyarlı polimerler, sıcaklık değişimiyle farklı davranış gösteren uyaranlara duyarlı polimerlerin veya akıllı malzemelerin bir sınıfıdır ve çoğunlukla iyonize edilemeyen makromoleküllerde görülür. Bu farklı davranışa yanıt olarak sıcaklık değişimine genellikle serbest polimer zincirlerinin konformasyonel değişimi veya çözünürlük değişimi olarak gözlemlediğimiz bir hacim fazı geçişi eşlik eder.

Isıya-duyarlı davranış, polimer-çözücü ve polimer-polimer segmentleri arasındaki intramoleküler ve intermoleküler etkileşimlerin birbirleriyle yarışından kaynaklanmaktadır. Hidrojen bağları açısından, üç yarışmalı etkileşim vardır: polimer-polimer, su-su ve polimer-su. Yüksek sıcaklıklarda, ısıya-duyarlı polimerler, hidrojen bağlarını , dipoller ve hidrofobik moleküller arasındaki etkileşimleri bozarak faz geçişine uğrar. Başka bir deyişle, ısıya-duyarlı polimerlerin faz geçiş sıcaklığı, etkileşimler arasındaki denge ile belirlenir.

Özellikle ısıya-duyarlı polimerler, polimerin faz diyagramının bu geçiş davranışını açıkça gösterdiği sulu çözeltilerde sıcaklığa bağlı karışabilirlik boşluğu sergiler. Bionadal olarak adlandırılan sınır eğrisi, bir fazlı bölgeyi polimer ve çözücünün karışmaz olduğu iki fazlı bölgeden ayırır. Eğrinin üst noktasına kritik sıcaklık (Tc) denir. Polimerler, sıcaklık değişiminin bir fonksiyonu olarak faz tepkilerine göre iki sınıfa ayrılır; birincisi, alt kritik çözelti sıcaklığı (LCST) adı verilen kritik bir sıcaklık ölçeğinin üzerinde çözünmez hale gelen polimerler ve ikincisi, üst kritik çözelti sıcaklığı (UCST) adı verilen kritik bir sıcaklık ölçeğinin altında çökelen ve faz değişikliklerine uğrayan polimerler.

Faz geçiş sıcaklığı birçok faktörden etkilenebilir. Tuz, yüzey aktif maddeler, ko-çözücüler gibi katkı maddeleri bunlardan birkaçıdır. Bu katkı maddelerinin etkisi genellikle çözeltinin çözücü kalitesini değiştirmesine sebep olur ve sonuç olarak polimerin hidrojen bağlanma kabiliyeti de dahil olmak üzere polimer-çözücü etkileşimleri değişir. Özellikle, yüzey aktif maddeler gibi amfifilik moleküller, polimerlere adsorbe olur ve polimerin hidrofilikliğini değiştirir. Polimer-polimer

etkileşimini, dolaşıklıklarını, çapraz bağlamayı veya dallanmayı artıracak polimerlere hidrofobik yapıların dahil edilmesi veya fonksiyonel grupların eklenmesi, karışımın entropisi (ΔS) ve entalpisini (ΔH) ve sonuç olarak polimerin ısıya-duyarlı davranışını etkileyecektir

Düşük kritik çözelti sıcaklığında (LCST) yumaktan-küreciğe faz geçişini sergileyen ısıya duyarlı polimerler, akıllı malzemelerin geliştirilmesinde büyük ölçüde ilgi toplayan bir konu olmuştur. Sulu çözeltilerdeki LCST davranışının bir sonucu olarak, polimerler ısıtıldıktan sonra sudan ayrılır, bu da çözünürlüğün azalmasına ve seyreltilmiş çözeltiler için hidratlanmış yumaktan çökmüş küreciğe konformasyonda bir değişikliğe neden olur. Basitçe açıklamak gerekirse, polimer, hidrojen bağları ve polimer ile su arasındaki sınırlı etkileşimleri nedeniyle LCST altında suda çözünür, ancak ısıtıldıktan sonra su ve polimer arasındaki etkileşimler bozulur, polimer intramoleküler etkileşimler baskın olur ve polimer fazı sudan ayrılır.

LCST davranışı büyük ölçüde, hacim geçişinin iyon konsantrasyonu ile ilişkili olduğu yükler arasındaki ortalama zincir uzunluğu tarafından kontrol edilir. LCST'yi etkileyen faktörler için genel bir kural olarak, polimer-polimer etkileşimlerini destekleyen her faktör LCST'yi düşürür, ancak polimer-su etkileşimlerini veya polimerin çözünmesini destekleyen her faktör LCST'yi yükseltir. Başka bir deyişle, LCST, çözeltilerdeki polimer-polimer, polimer-su veya su-su etkileşimlerinin ayarlanmasıyla kontrol edilebilir. Polimer yapısının kopolimerizasyon yoluyla modifikasyonu, yan grupların eklenmesi veya uç grupların modifikasyonu, seçilen polimerin LCST'sini ayarlamak için bazı örneklerdir. LCST değeri, çözeltideki polimer konsantrasyonu arttıkça azalır. Ayrıca, çözeltideki tuzlar polimerin LCST değerini azaltır. Polimer zincir uzunluğundaki bir artış veya çözeltideki konsantrasyonu, termo-duyarlı polimerler için LCST değerini azaltır.

Bu çalışmada, sulu çözeltilerdeki ısıya-duyarlı polimerler incelenmiştir, çünkü konformasyonel değişiklikler fonksiyonel grupların rolünü ve su ile etkileşimlerini belirlemede çok kritik bir rol oynamaktadır. Yoğunluk Fonksiyoneli Kuramı (YFT) kullanılarak yapısal değişiklikleri incelemek için suda LCST davranışı sergileyen poli(N-izopropilakrilamid (PNIPAAm), poli(N-vinilizobütiramid) (PNVIBA) ve poli(2-etoksietil vinil eter)(PEOVE) kullanılmıştır. Hesaplamalar, organik molekül yapılarının iyileştirilmesinde en iyi performans gösterdiği bilinen B3LYP fonksiyoneli ve 6-31G (d, p) baz seti kullanılarak gerçekleştirildi. Bu monomerlerin dimer moleküllerinden başlayarak optimize edilmiş en uzun oligomer zinciri olan pentameriyle su molekülünün hidrojen bağı etkileşimi çeşitli konfigürasyonlar test edilerek modellenmiştir. Etkileşim enerjileri B3LYP, LC-wPBE ve CAM-B3LYP fonksiyonelleri kullanılarak, 6-311G(3df,2pd) baz setinde hesaplandı. Hidrojen bağının nicel bir yorumu için tüm etkileşim enerjisi hesaplamalarında baz seti üst üste binme hatası (BSSE) hesaba katıldı. Bulunan etkileşim enerjilerine sıfır noktası enerjisi düzeltmesi (ΔZPE) de dahil edildi.

Segment···· çözücü ve segment····segment etkileşimleri, çözeltilerde polimer zincir konformasyonu üzerindeki etkileri açısından araştırılmıştır. Oligomer zincir büyüklüğünün konformasyon üzerine etkisi de çalışıldı. Ana zincirdeki konformasyon değişimini gözlemlemek için, oligomer-su kompleksleri ile susuz oligomer zincirleri arasında dönme yarıçapı (Rg) ve kare ortalama karekök sapması (Rmsd) hesaplandı.

Bu çalışmadaki hesaplamalar, ısıya duyarlı polimerlerin tek zincirlerdeki konformasyonel geçişde moleküler arası etkileşimlerin etkisi üzerinde fikir vermeyi

amaçlamıştır. Hesaplamalarımıza göre, su molekül sayısının artışı moleküler arası etkileşimlerin kuvvetlenmesine neden olmuştur.

1. INTRODUCTION

1.1 Smart or Stimuli-Responsive Materials

The term "Smart" or "stimuli-responsive material" refers to materials that are capable of responding to external stimuli and changes in their environment (Teotia et al., 2015). Polymeric materials are cheaper and easier to work with than ceramics and metals, making them a part of the main group of "smart" materials (Ward et al., 2011). Polymeric "smart" materials are capable of significantly altering their physicochemical properties when exposed to physical factors (pressure, temperature, light, sound, electrical and magnetic fields), chemical factors (pH, solvent composition, ionic strength), and/or biological factors (enzymes, receptors) (Kumar et al., 2007; Leszczynski et al., n.d.; Zhelavskyi & Kyrychenko, 2019). As a result of external stimuli, smart polymeric solutions respond in several different ways. Physical stimuli change the chain dynamics and the energy level of the polymer-solvent system. Chemical stimuli affect intermolecular interactions, whereas biological stimuli alter the function of molecules (Leszczynski et al., n.d.) (James et al., n.d.). As a result of altering molecular interactions caused by external stimuli (temperature, pH, mechanical, electric, or magnetic fields, etc.), the levels of various interaction energies vary. The hydrophilic-hydrophilic balance in these materials can result in reversible microstructural changes (Aguilar & San Román, 2019; Taylor & Cerankowski, 1975; Teotia et al., 2015). As a result of the ability to control polymer systems by external stimulus, "smart" polymers have been used in a variety of applications, including tissue engineering, drug delivery, sensors, and gene delivery. In recent years, there has been an increase in the demand for functional, smart systems that has led to an increasing

1.1.1 Thermo-Responsive polymers

As a class of "smart" materials, thermo-responsive polymers undergo a rapid change in their solubility with a small decrease in temperature (Gobeze et al., 2020; James et al., n.d.). Since temperature can be easily applied from the outside, the changes in temperature represent unique stimuli among the present stimuli. It has been

demonstrated that thermo-responsive polymer systems are most often constructed with non-ionizable macromolecules (Schattling et al., n.d.). In general, thermo-responsive polymers dissolve in water at low temperatures and are transparent. With increasing temperatures, they undergo a reversible phase transition that results in either a cloud or precipitate ("Encyclopedia of Polymeric Nanomaterials," 2015; Ghizal et al., 2014). The mechanism triggers the coil-to-globule transition or volume phase transition (VPT) by disrupting hydrogen bonds and/or interactions between dipoles and/or hydrophobic molecules (Flemming et al., 2021; Leszczynski et al., n.d.). Polymers are classified into two classes based on their phase response as a function of temperature change; first, polymers that become insoluble above a critical temperature scale called the lower critical solution temperature (LCST), and second, polymers that precipitate below a critical temperature scale called the upper critical solution temperature (UCST) and undergo phase changes (Flemming et al., 2021; Roy et al., 2013a).

When a polymer exhibits UCST behaviors, it separates from the solution below the critical solution temperature. However, as the temperature rises, it becomes soluble UCST behaviors are usually observed in organic solvents or water/organic solvent mixtures. A representative UCST-type thermo-responsive polymer is shown in Figure 1.1. The behavior of UCST is controlled by enthalpy, as there are stronger polymer-polymer interactions and solvent-solvent interactions than weak polymer-solvent interactions (Flemming et al., 2021; Roth et al., 2013).

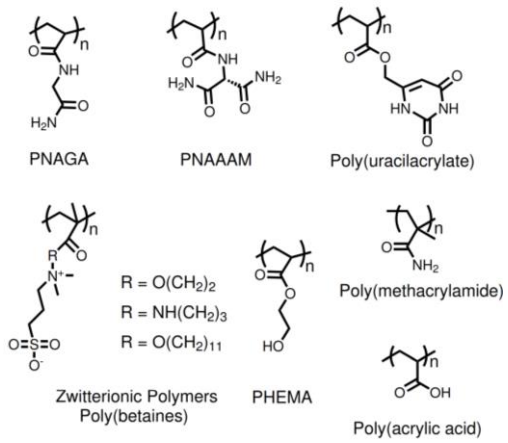

Figure 1.1: Chemical structures of UCST- type polymers (Teotia et al., 2015)

Most commonly used LCST thermosensitive polymers include poly(N-isopropyl acrylamide), poly(N-vinylalkylamide), PLGA–PEG–PLGA triblock copolymers, poly(N, N-dimethyl acrylamide), poly(N-vinyl caprolactam), phosphazene derivatives, polysaccharide derivatives, and chitosan (Leszczynski et al., n.d.). Figure 1.2 illustrates examples of LCST-type polymers.

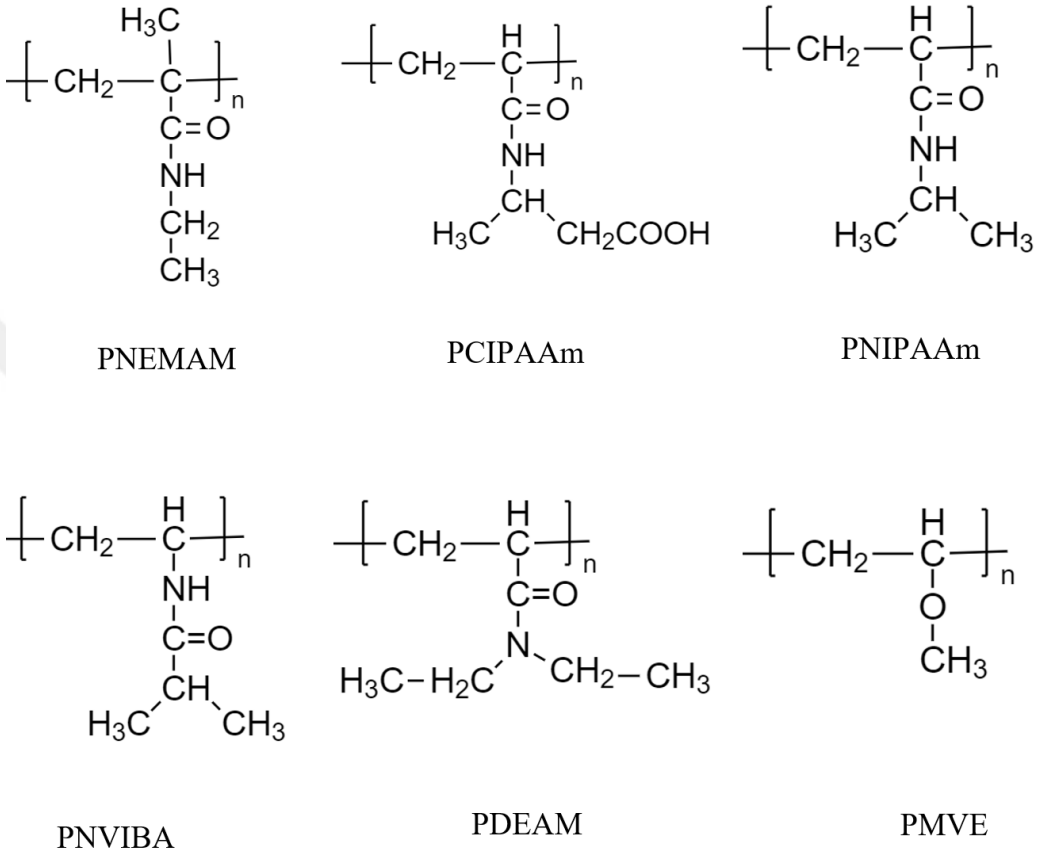

Figure 1.2: Representative LCST polymers and their chemical structures

As a result of the lower critical solution temperature (LCST), the polymeric system becomes hydrophobic and insoluble, leading to phase separation. At normal temperatures, thermo-sensitive polymers exhibiting LCST behavior are completely miscible; however, their solubility decreases as the temperature increases and they exhibit phase separation over the critical solution temperature, which indicates that a temperature stimulus causes phase separation in the polymer system. Accordingly, when the temperature of an aqueous solution of LCST exhibiting thermo-responsive polymer increases, the polymer chains undergo a transition from coils to globular to aggregates in Figure 1.3. Hydrogen bonding and hydrophobic interactions in the polymer-solvent system contribute to phase transitions and the transition from

hydrated random coils to hydrophobic globular above critical solution temperatures (Gobeze et al., 2020; Roy et al., 2013a; Teotia et al., 2015).

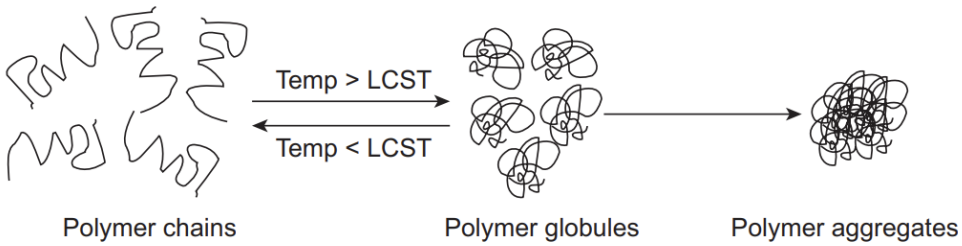

Figure 1.3: a) polymer chains b) polymer globules c) polymer aggregates

A hydrophobic-hydrophilic transition triggered by temperature can be reversed and the polymer solution can be cooled to return it to its original state. LCST is frequently observed in highly polar media such as water or alcohol, as hydrogen bonds are formed in polymer-solvent interactions (Schattling et al., n.d.).

1.1.1.1 Poly(N-Isopropylacrylamide) (PNIPAAm)

The thermo-responsive properties of water-soluble poly(N-vinylalkylamide) based polymers are remarkable (Roy et al., 2013a). Due to their unique thermo-responsive behavior in aqueous media, N-substituted acrylamides are an extensive class of thermo-responsive polymers. The poly (N-isopropyl acrylamide) (PNIPAAm) in Figure 1.4 included in this class is one of the most studied thermosensitive materials both experimentally and computationally. It is obtained by polymerizing the N-isopropyl acrylamide (NIPAAm). For PNIPAM, the lower critical solution temperature (LCST) is typically around 305 K in water (Abbott & Stevens, 2015; Ortiz De Solorzano et al., 2020). When the temperature is raised above the lower critical solution temperature (LCST), PNIPAAm can undergo a coil-to-globule transition. The conformational change in PNIPAAm illustrated in a schematic diagram in Figure 1.5.

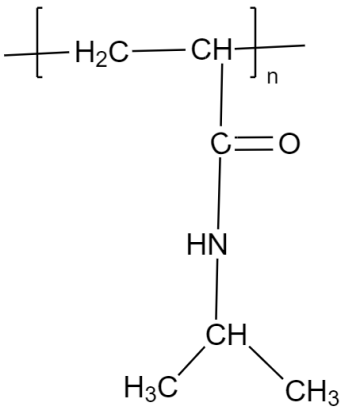

Figure 1.4: Chemical structure of PNIPAAm

Several studies have examined the LCST of the PNIPAAm in order to understand a coil-globular transition (Alaghemandi & Spohr, 2013; Azmi et al., 2018; S. Deshmukh et al., 2009; S. A. Deshmukh et al., 2012, 2014; Kamath et al., 2013). A 50-unit oligomer model was simulated in 2004 by Longhi et al. (Longhi et al., 2004) for the thermo-responsive polymer poly(N-isopropyl acrylamide in a diluted aqueous solution at 300 and 310 K.

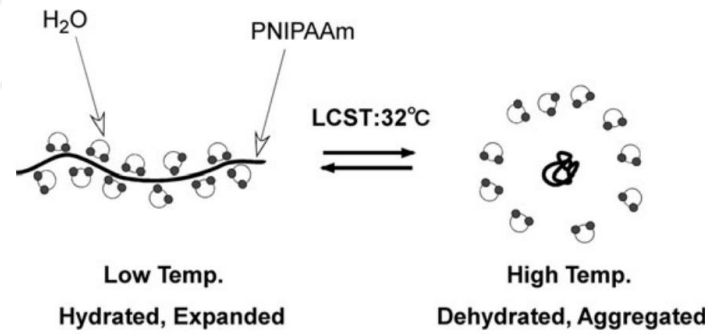

Figure 1.5: Conformational change in PNIPAAm, a)expanded b)aggregated

This is one of the first MD simulations conducted for PNIPAAm-water systems. According to Longghi et al. (2004), the first hydration shell is primarily located in the hydrophilic region of the monomer when hydrogen bonding occurs**.**

PNIPAAm includes hydrophobic $–CH_2–CH_2–$ and $–CH–(CH_3)_2$ groups laid out in its backbone and side chain, respectively and the hydrophilic –N–H and C═O groups laid out in its side chain. Below LCST, hydrogen bonds between hydrophilic groups in polymers and water molecules exhibit extended chain conformations. The hydrogen bonds formed between N–H or C═O groups of the polymer and water around the polymer chains break as the temperature of the polymer solution approaches its

transition point, collapsing the polymer molecule and forming a hydrophobic globule. In addition, as the temperature increases, the remaining hydrogen bonds also break, resulting in hydrophobic interactions dominating the polymer chains due to the dehydration of the hydrophobic isopropyl group. Furthermore, above critical solution temperatures (CST), PNIPAAm's backbone folds onto itself to conserve hydrophobic groups from water, causing the polymer to aggregate and separate from the solution

(Lanzalaco & Armelin, 2017; Leszczynski et al., n.d.; Ortiz De Solorzano et al., 2020; Qiu & Park, 2001; Teotia et al., 2015).

The thermosensitivity of PNIPAAm can easily be modified by modifying the side chains or by incorporating co-monomers with different hydrophilic/hydrophobic values (Kuckling et al., 2000). Furthermore, the LCST value of PNIPAAm can be adjusted by adding a co-monomer, and the nature of the co-monomer will determine the LCST value. Hydrophobic compounds lower the LCST value, whereas hydrophilic compounds raise it. As an example, by copolymerizing hydrophobic (N-tert butylacrylamide) with hydrophobic (NIPAAm), the LCST is reduced by 10 °C, and it is further reduced by increasing the composition of (N-tBAAm). Nevertheless, the LCST of the copolymer of hydrophilic dimethyl acrylamide (DMAAm) and (NIPAAm) was increased from 32 °C to 45 °C by increasing DMAAm composition ("Encyclopedia of Polymeric Nanomaterials," 2015). Copolymerization of hydrophilic and hydrophobic monomers results in changes in the segmental mobility of a polymer chain. Because of increased segmental mobility and flexibility, water is readily able to penetrate the chain even at temperatures above the critical solution temperature (CST) as a result. Alternatively, the size of the side groups, architecture, and molecular weight of the molecule, as well as the concentration of polymer in solution should be considered when determining the LCST value of a polymer (Ward et al., 2011).

The LCST value of PNIPAAm decreases as the polymer concentration in the solution increases. Furthermore, salts in the solution reduce the LCST value of the polymer. An increase in polymer chain length or its concentration in solution reduces the LCST value for PNIPAAm. Moreover, salts in the solution decrease the LCST of the polymer. Due to its solubility in water and LCST-body temperature, PNIPAAm is widely used in pharmaceutical delivery systems and tissue engineering for regenerative medicine (Flemming et al., 2021; Roy et al., 2013a; Ward et al., 2011).

1.1.1.2 Poly(N-vinylisobutyramide) (PNVIBA)

The thermo-responsive properties of Poly(N-vinylisobutyramide) (PNVIBA) which is a water-soluble poly(N-vinylalkylamide) based polymer are remarkable. PNVIBA in Figure1.6 is a polymer synthesized from N-vinylisobutyramide (NVIBA), a derivative of N-vinyl acetamide (NVA) by Akashi et al. (Roy et al., 2013a, 2013b).

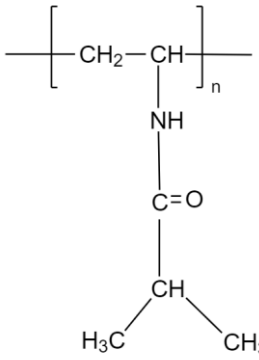

Figure 1.6: Chemical structure of PNVIBA

A structural isomer of PNIPAAm, poly(N-vinylisobutyramide) (PNVIBA), exhibits a sharp thermal transition at 39°C (Suwa et al., 1997), but the cloud point is strongly influenced by the concentration of the polymer in solution. In addition, the cloud point of PNVIBA solutions decreases linearly as salt concentration increases. The hydrophilic-hydrophobic balance of PNVIBA is similar to PNIPAM, but the transition temperature is higher, which may be due to the microstructure of the hydrated polymer (Roy et al., 2013a).

1.1.1.3 Poly(Oxyethylene Vinyl Ether) (PEOVE)

Poly(vinyl ether) containing an oxyethylene side chain was synthesized by Aoshima, and the thermosensitivity of the polymers in an aqueous solution was demonstrate (Aoshima et al., n.d.). Poly(2-ethoxyethyl vinyl ether)(PEOVE) exhibiting phase transition at 20 °C is a poly(oxyethylene vinyl ether) based polymer in Figure 1.7.

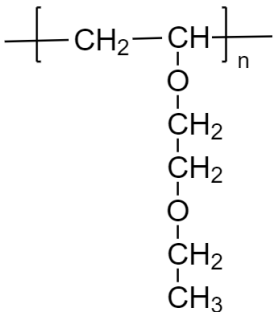

Figure 1.7: Chemical structure of PEOVE

Thermo-responsive poly(vinyl ether)s precipitate as a result of hydrophobic interaction at higher temperatures above the LCST-type phase separation temperature. The polymers with smaller polydispersity index exhibited sharp phase separation behavior when temperature changes occurred. Furthermore, the behaviour of phase separation differed among polymers with the same monomer composition but different sequence distributions, such as random, diblock, and triblock polymers. By using systematically prepared poly(vinyl ether), it is also possible to achieve a thermoreversible sol-gel transition and to control gelation capability ("Encyclopedia of Polymeric Nanomaterials," 2015).

1.2 Polymer in Solutions

An understanding of polymer solution thermodynamics is based on understanding what happens physically when the polymer is dissolved in a solvent with a low molecular weight. Initially, the solvent molecules slowly diffuse into the polymer, resulting in a swollen gel. If the polymer-polymer interactions are high, for example, due to cross-linking or strong hydrogen bonds, then that will be all that occurs. Alternatively, if the interaction between a polymer and a solvent is high enough, then the gel disintegrates and the polymer dissolves to form a "true" solution. Once the polymer is dissolved, it usually takes the form of a random coil mass whose conformations occupy a volume many times greater than that of its segments alone.

When a solvent is good, interactions between polymer segments and solvent molecules are energetically favorable, which will cause polymer coils to expand. When the solvent is poor, polymer-polymer interactions are preferred, and the polymer coils will contract. Solvent quality is determined by the chemical composition of both the

polymer molecules and the solvent molecules, as well as the temperature of the solution.

In a solvent, a real polymer chain behaves as an ideal chain at a temperature known as theta temperature (T_θ). Polymer segments act as ideal chains at the theta temperature because the attractive interactions between them compensate for the repulsive interactions caused by the excluded volume effect. Low temperatures (below T_θ) create collapsed polymer segments, which is why the solvent is called poor at these temperatures. Additionally, as a result of the repulsive interaction between the polymer segments, polymers at higher temperatures have more extended conformations, and the solvent at these temperatures is considered a good solvent (Katsumoto et al., 2002; Leszczynski et al., n.d.; Teraoka, 2002). Figure 1.8 illustrates how temperature affects the behavior of a real chain and how an ideal chain behaves at the T_θ temperature.

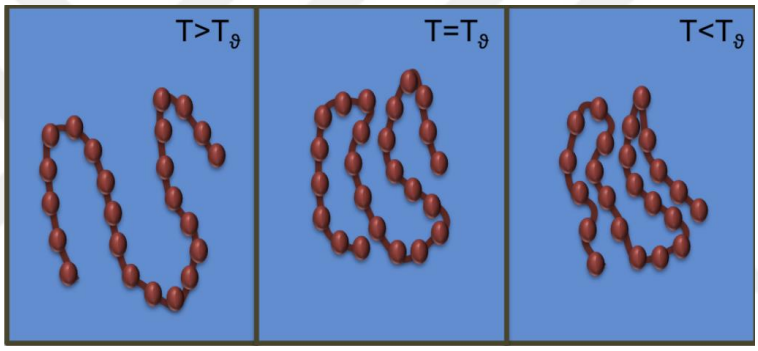

Figure 1.8: The effect of T_θ on the conformational structure of polymers

1.3 Polymer Conformational Structure Overview

Many scientists have been interested in the conformational changes of polymers due to the fact that the microscopic structures of polymers influence their macroscopic properties. A polymer's conformation is generally affected by two types of interactions: short-range interactions and long-range interactions. The concept of short-range interactions refers to interactions between chain units that are physically close to one another in terms of the path of the random walk, whereas long-range interactions refer to interactions that are spatially close but may involve chain units that are positioned at a distance from one another. The short- and long-range interactions both involve chain units that are spatially close to each other as shown Figure 1.9. It is believed that these interactions are derived from van der Waals interactions, chemical bonds between side chains (such as hydrogen bonds and

disulfide bonds), an affinity between polymers and solvents (such as hydrophobic interactions), electrostatic interactions (such as electric dipoles and electrolytes), and topological interactions (such as entanglements). A polymer's coil-globule transition is thought to be caused by these interactive forces (Katsumoto et al., 2002).

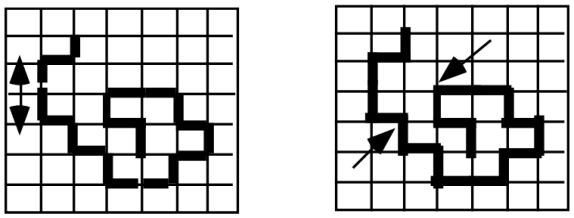

Figure 1.9: Representation of the short (left) and long-range (right) interactions

A polymer chain can exist in any of its possible configurations, including tight coils and straight chains. There are many possible conformations that would achieve a given end-to-end distance, so its likelihood increases. A straight-chain can only be formed by one conformation, but as the molecule becomes more coiled, the number of conformations increases. As a result, a polymer chain tends to coil up to a certain extent. An end-to-end chain distance can be estimated by considering a molecule as being composed of n segments, where n is the number of segments in the molecule. The segments are rigid but are freely jointed at both ends so that they can form any angle with their neighboring segments. In order to construct a model molecule, each successive segment can be added at a random angle, called a random walk. A random walk may cross itself several times, but if it does not penetrate itself, a self-avoiding walk is formed (Teraoka, 2002).

It is possible to construct a random walk more easily using a lattice, where the choice of direction is limited and the step length is fixed. A lattice can also be used for a self-avoiding walk(Figure 1.10).

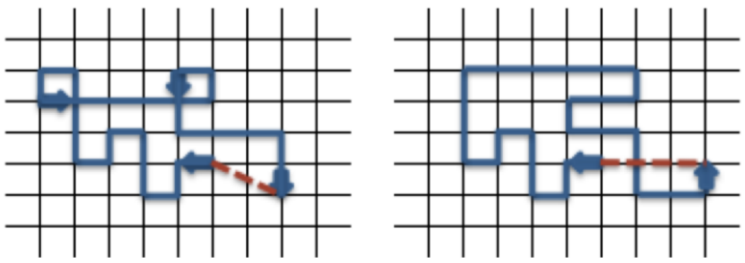

Figure 1.10: Representation of the random walk (left) and the self-avoiding random walk (right)

Given the Kuhn length and the number of segments in a molecule modeled by a random walk, we are able to estimate the distance between the ends of the molecule. A vector represents each segment . $\overrightarrow{r_n}$(Figure 1.11).

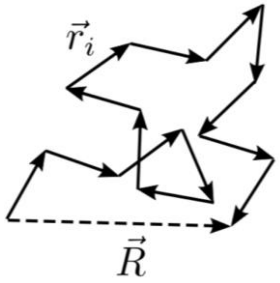

Figure 1.11: Vector representation of each segment in a chain

The effective length of the freely joined bonds on a bond on a polymer chain is known as the Kuhn Length (b). It is a constant that is determined by the solvent's and polymer's chemical compositions (Birshtein & Buldyrev, 1991. In the Kuhn segment chain, the length of a fully stretched chain is L and calculated by L = N b. According to the random walk model, R, the average end-to-end distance for a chain is R =N.b

$$\langle R^2 \rangle = Nb^2 \qquad \textbf{(1.1)}$$

The effective length of the freely joined bonds on a bond on a polymer chain is known as the Kuhn Length (b). It is a constant that is determined by the solvent's and polymer's chemical compositions (Birshtein & Buldyrev, 1991).

1.4 Interactions in Polymer Chains

Intermolecular forces may be classıfield into two parts as attraction and repulsion forces. Attraction forces depend on the interparticle distance in n.th power inversely (R^{-n}). These forces are of long range and, in general, orientation dependent. Electrostatic forces(ion-dipole, dipole-dipole), induction (dipole – induced dipole) and dispersion (induced dipole – induced dipole) forces are known as the type of atraction forces. On the other hand, repulsion forces are of short range exhibiting exp (-βR) depence on the interparticle distance and mostly of Pauli repulsion. There also exist some complex interactions such as van der Walls (sum of dipole-dipole, dipole -induced dipole and dispersion forces), $\pi - \pi$ stacking and hyrogen bonding which have mostly an electrostatic character and highly directional.

Hydrogen bonds (H-bonds) are the result of dipole-dipole forces between strongly electronegative atoms (e.g., fluorine (F), nitrogen (N), oxygen (O)), and hydrogen atoms. The hydrogen bond is usually represented by X— H……Y and it is the result of the interaction between a proton-donating bond X-H and a proton acceptor Y, where X and Y represent electronegative atoms such as O, N, and Cl. So, we can consider O—H…O, N—H…N, N—H…O, N—H…Cl and similar systems are typical, conventional hydrogen bonds (Grabowski, 2004).

Having an understanding of the role of hydrogen bonding interactions is crucial since they influence the physical properties and microstructures of many materials. For example; PNIPAAm exhibits a unique volume phase transition from a hydrated state known as a hydrophilic state with an expanded structure to a shrunken dehydrated state known as a collapsed structure at a critical temperature. The LCST is primarily influenced by the hydrogen bonding between water molecules and the structure of the functional monomer units of PNIPAAm; that is, the C=O and N–H links.There is no doubt that the intermolecular force between highly electronegative atoms (e.g., N, O, F, and Cl) and hydrogen atoms play an important role, particularly in small organic molecules, inorganic acids, or among water molecules. During the dissolution of a polymer in water, three kinds of interactions can take place: interactions between polymer molecules, interactions between polymer chains and water molecules, and interactions between water molecules alone.

In addition to hydrogen bonding, the nature of intermolecular and intramolecular interactions in PNIPAAm solutions is sensitive to both temperature changes and the nature of the solvent. The interaction between the PNIPAAm molecules and solvents can thus be distinguished into two types: (i) pure water and (ii) a mixture of water and organic solvents. At transition temperature (32°C), PNIPAAm aqueous solutions become abruptly turbid and easily switch to a liquid state when the temperatures fall below that level. Figure 1.12 illustrates the stabilization of the collapsed state when PNIPAAm changes from its liquid to an almost solid state. This behavior is based on the number and types of hydrogen-bonding interactions upon switchable response (Grabowski, 2004; Jeffrey, 1996; Lanzalaco & Armelin, 2017).

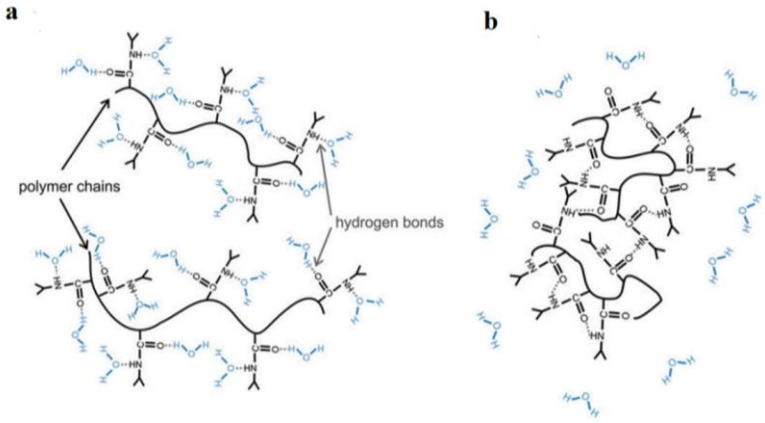

Figure 1.12: (a) PNIPAAm hydrogel swollen in aqueous solution below Tc (32 °C) (b) dehydrated PNIPAAm hydrogel shrunken above Tc (32 °C) (Lanzalaco & Armelin, 2017)

The interactions between nearby monomers, known as short-ranged interactions, and monomers separated by a great distance, known as long-ranged interactions, determine the chain configurations. The covalent bonds between a polymer's monomers, which stand in for short-range interactions, determine how flexible it is. The prevalence of particular polymer conformations is determined by long-range interactions between polymer segments that are positioned considerably apart along the polymer chain backbone. A sign of long-ranged interactions that prevent two polymer segments from occupying the same space location is the excluded volume effect. The incompressibility restriction limits the sum of the volume fractions of the components in a mixture. Furthermore, the interactions between the polymer segments from the same chain, different chains, and the surrounding molecules, such as solvent molecules, can be either attractive or repulsive. The polymer conformations are impacted by these interactions, such as van der Walls, hydrogen bonding, and dipole-dipole interactions and so on (see section 1.3 polymer conformational structure overview).

Van der Waals attraction between molecules is the result of the presence of induced electric dipole moments on a nearby nonpolar molecule, which corresponds to the effective separation of charges within the molecule, resulting in a van der Waals attraction between molecules. An induced polar molecule is likely to attract other polar molecules, resulting in a special type of interaction. This interaction can be observed in polymer mixtures between unbound monomers or between solvent molecules. The van der Waals forces in a system are disrupted by normal thermal molecular motion.At

lower temperatures, Van der Waals forces become more effective at ordering molecules, leading to polymer condensation. Thermal motion declines with decreasing temperature, so van der Waals forces become more effective in order to keep the molecules in place.

1.5 Thermodynamic Behavior of Polymer Solutions

It is necessary to understand the thermodynamic picture to predict the thermo-responsive behavior of the polymer. At the reaction conditions, Gibbs free energy (ΔG) must be negative for a process to be thermodynamically feasible. As mentioned above, a variety of interactions occur between polymers and solvents during polymer dissolution. Consequently, all of these interactions would result in negative values for enthalpy and entropy for spontaneous dissolution of the polymer in a solvent, producing a homogeneous system. If the value for (ΔG) is positive at a certain temperature for a polymer-solvent system, then the polymer will not be miscible with the solvent, and two different phases will exist.

$$\Delta G = \Delta H - T\Delta S \qquad \textbf{(1.2)}$$

Polymers with LCST behavior exhibit negative Gibbs free energy at normal temperatures and are soluble in aqueous solutions. A thin layer of water molecules forms around the hydrophilic part of the polymer, which contributes to the negative enthalpy of the dissolution process. Water molecules form a structured arrangement around the hydrophobic part of a polymer. These water molecules form extensive hydrogen bonds, thereby reducing the reaction's entropy (ΔS). The entropy of the aqueous polymer system increases as the temperature is raised, which results in hydrogen bonds breaking, causing the hydration shell to collapse. In this case, the entropy of the system increases more than the negative enthalpy of the reaction, giving a positive value to Gibbs free energy. Hydrophobic interactions increase when hydrogen bonds are broken and hydration shells are lost. Consequently, chain collapse and intermolecular aggregation lead to the separation of polymer chains into two phases, suppressing conformational changes of polymer chains. The enthalpy and entropy of UCST polymers are positive, decreasing with increasing temperature, showing opposite behavior to that of LCST polymers (Imberg, n.d.; Teotia et al., 2015).

1.5.1 Flory-Huggins theory

The Gibbs free energy of mixing ΔGm must be negative for a polymer-solvent binary mixture to result in a homogeneous solution (see section 1.5). There are two main contributions to the Gibbs free energy density: an entropic part resulting from the variety of polymer chain configurations, and an enthalpic part resulting from interactions between polymer-solvent (p-s), polymer-polymer (p-p), and solvent-solvent (s-s).

According to Flory-Huggins theory [FH], the Gibbs free energy of mixing is:

$$\Delta G_m = RT[\varphi_1 N_1 \ln\varphi_1 + \varphi_2 N_2 \ln \varphi_2 + \chi\varphi_1\varphi_2] \quad \textbf{(1.3)}$$

where the volume fractions of the two species in the binary mixture are φ1 and φ2, respectively. Consider that (φ1 + φ2) = 1. The number of lattice sites occupied by each type of molecule is defined by N1 and N2, and the Flory-Huggins interaction parameter is represented by χ. The FH equation for polymer solutions seems like this when N1 = N and N2 = 1 are substituted. A contribution from entropy is represented by the first two terms, and an energetic contribution is represented by the last term. For polymer–solvent systems, the entropy of mixing is small at low concentrations, which is why the change in interactions upon mixing determines the miscibility. Typically, we are considering short-range interactions here, including van der Walls interactions (also known as dispersions), hydrogen bonds, and dipole-dipole interactions. The difference in interaction energies in the mixture is described by the dimensionless quantity known as the Flory-Huggins interaction parameter [χ]. To forecast the phase diagram of the mixture, it is essential to understand the value of the Flory interaction parameter[χ].

On the basis of the equation developed by Hildebrand and Scott, the χ for non-polar mixtures can be predicted as follows:

$$\chi \approx \frac{V_0(\delta_1-\delta_2)^2}{RT} \quad \textbf{(1.4)}$$

where V_0 is the molar volume of the polymer chain segment, δ1 and δ2 are the Hildebrand solubility parameters. Eq.(1.4) is more frequently used to describe non-polar polymer solutions, which have constant and positive χ values independent of temperature (Kuckling et al., 2012; Leszczynski et al., n.d.).

1.5.2 Phase behavior of polymer solutions

It is well known that temperature-responsive polymers exhibit a miscibility gap that is influenced by temperature in aqueous solutions. Within the miscibility gap, the mixture splits into two composition phases, one polymer-rich and another solvent-rich. (ϕ', ϕ'')

The binary mixture phase diagram of these polymers clearly demonstrates this transitional behavior. The phase diagram is characterized by the spinodal and binodal curves, as well as the critical point. Spinodal curves represent the limit of thermodynamic stability for single-phase mixtures, whereas binodal curves represent the extent of the stable, homogeneous region. At the critical intersection of the spinodal and binodal lines, where :

$$\partial^2 \mathrm{G} / \partial \phi^2 = \partial^3 \mathrm{G} / \partial \phi^3 = 0 \qquad \textbf{(1.5)}$$

The two lines come together. Figure 1.13 illustrates the conformational changes of polymers in one- and two-phase regions. The critical point is the extremum point of the boundary curve. These characteristics are strongly influenced by the interaction parameter$[x]$.

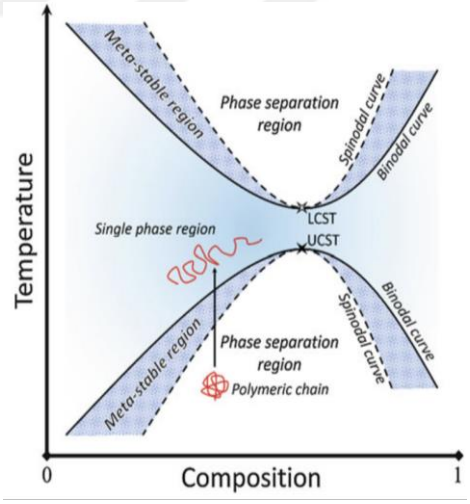

Figure 1.13: LCST and UCST phase diagrams for polymer solutions (Flemming et al., 2021)

The most common empirical form of x(T) is as follows:

$$x(\mathrm{T}) = \mathrm{a} + \frac{\mathrm{b}}{\mathrm{T}} \qquad \textbf{(1.6)}$$

In this form, a and b experiment constants. It is generally assumed that results from local entropic factors and b from enthalpic factors. Accordingly, for the simplest case where$[x]$ varies inversely with T, a and b have values greater than zero.

In the case of positive b and $[x]$ decreasing with T, the polymer mixture will be phase-separated at low T and become homogeneous as T increases. In phase behavior, this phenomenon is referred to as upper critical solution temperature or UCST. The converse case, where b is negative, results in lower critical solution (LCST) phase behavior (Figure 1.14). As a result, the polymer mixture is homogeneous at low temperatures and separates into phases upon heating (Flemming et al., 2021; Imberg, n.d.).

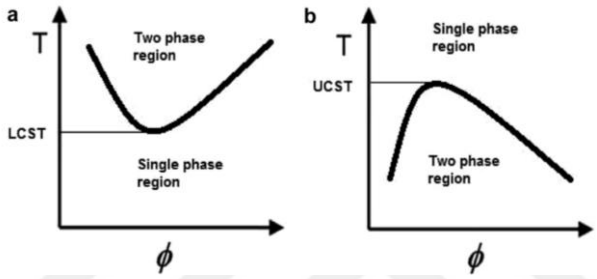

Figure 1.14: Temperature vs. polymer volume fraction. (a)LCST (b)UCST behaviour (Ward et al., 2011)

The purpose of this master's thesis is to provide insight into the effect of intermolecular interactions on conformational transitions in single chains of thermo-responsive polymers. To this end, Poly (N-isopropylacrylamide) (PNIPAAm), Poly(N-vinylisobutyramide) (PNVIBA), and poly(2-ethoxyethyl vinyl ether)(PEOVE) exhibiting LCST behavior in water were studied to examine structural changes by using DFT. The hydrogen bond interaction of the water molecule with the pentamer of these monomers was modeled by testing various configuration.

2. THEORY

The term theoretical chemistry refers to the mathematical description of chemistry. On the other hand, Computational chemistry refers to the application of mathematical methods to chemistry which can be automated for implementation on a computer through the use of automata. There is no mention of the words "exact" or "perfect" in these definitions.There are very few aspects of chemistry that can be computed precisely, but almost all aspects of chemistry can be described in terms of a qualitative or approximate numerical computation.

The use of computational methods in chemistry has become useful for solving complex problems in order to help researchers predict the outcome of experimental investigations before they embark on them. As a result, computational chemistry helps researchers save time and money. It is based on quantum mechanics, classical mechanics, statistical mechanics, and thermodynamics. As molecules consist of nuclei and electrons, quantum mechanical methods are used to study them. The quantum mechanical calculation procedure typically utilizes ab initio, empirical, or semi-empirical approaches in order to solve a set of simplified Schrödinger equations (2.1).

$$H\Psi = E\Psi \qquad \textbf{(2.1)}$$

where Ψ is the wavefunction of the system, E is the energy of the system, and H is the Hamiltonian operator to determine kinetic and potential energy.

In principle, it is possible to solve the Schrödinger equation, either in its time-dependent form or in its time-independent form based on the problems at hand, but this is not possible in practice except for very small systems. Thus, a great number of approximate methods are designed to achieve the best balance between accuracy and computational cost. Molecular properties can be routinely and very accurately calculated using computational chemistry for molecules containing no more than 10-40 electrons. By using approximate methods, such as Density Functional Theory

(DFT), larger molecules that contain larger systems up to 1000 atoms can be computed (Lewars, 2011; Young, 2001).

Comptational chemistry is classified into non- emprical, semi-emprical and molecular mechanics (Figure 2.1). This section, however, focuses on only density functional methods.

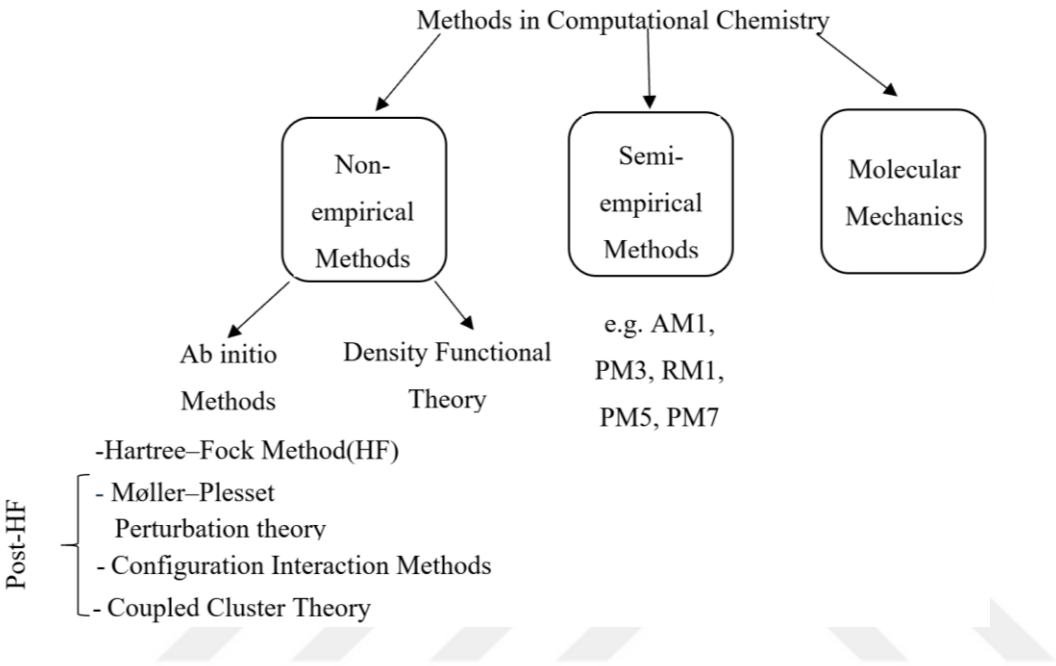

Figure 2.1: Methods in computational chemistry

2.1 The Density Functional Theory (DFT)

The Density Functional Theory (DFT)is based on the total electron density instead of the wave function. There is an approximate expression for the total electron density used in this type of calculation. DFT methods have the capability to provide relatively accurate results with low computational cost. There is no systematic way to improve the approaches by enhancing the functional form, in contrast to ab-initio methods.

DFT was first introduced by Hohenberg and Kohn in 1964, however, it only covered virtual functionals, while Kohn and Sham introduced the formal functionals based on total electron density in 1965. Kohn-Sham is the most common method for implementing density functional theory.

In density functional methods, the electronic energy is divided into several terms.

$$E = E_T + E_v + E_J + E_{xc} \qquad \textbf{(2.2)}$$

The kinetic energy is given by E_T, the potential energy of nuclear-electron attraction and nuclear-nuclear repulsion is given by E_V, and the electron-electron repulsion term is given by E_J. The exchange-correlation term, E_{XC}, includes the remaining electron-electron interactions, but the exact calculation of this therm not known.

Except for nuclear-nuclear repulsion, all terms are functionals of the electron density, $\rho(r)$. Exchange functionals and correlation functionals are two categories for E_{XC}. As a result of the antisymmetry of the quantum mechanical wavefunction and the dynamic correlation in electron motion E_{XC} represents the exchange-correlation energy.

In terms of electron density, the variational principle determines the ground state energy and electron density. Moreover, the ground state electron density $\rho(r)$ determines the external potential $v(r)$ as well as the ground state properties of the system of interest in a variational manner.

Electronic energy can be expressed as a functional of electron density:

$$E[\rho] = \int v\rho(r)dr + T[\rho] + V_{ee}[\rho] \qquad \textbf{(2.3)}$$

where $V_{ee}[\rho]$ represents interelectronic interactions and $T[\rho]$ represents the kinetic energy of interacting electrons.

In terms of electronic energy, the Kohn-Sham approach may be applied.

$$E[\rho] = \int v(r)\rho(r) + T_s[\rho] + J[\rho] + E_{xc}[\rho] \qquad \textbf{(2.4)}$$

This approach relies on an orbital density description which eliminates the need to know the exact form of $T[\rho]$. According to Kohn-Sham, the kinetic energy of a non-interacting system of electrons $Ts[\rho]$ should be viewed as a functional of a set of orbitals describing the exact density of a particle.

$$Ts[\rho] = \sum_{i=1}^{N} \left\langle \Psi i \left| -\frac{1}{2}\nabla^2 \right| \Psi i \right\rangle \qquad \textbf{(2.5)}$$

$J[\rho]$ indicates electron-electron repulsion (Coulomb energy), and $E[\rho]$ indicates exchange-correlation energy, with its functional derivative, called exchange-correlation potential),$v_{xc}(r)$.

$$E_{xc}[\rho] = T[\rho] - T_s[\rho] + V_{ee}[\rho] - J[\rho] \qquad \textbf{(2.6)}$$

$$v_{xC}(r) = \frac{\partial E_{xC}[\rho]}{\partial \rho(r)} \qquad \textbf{(2.7)}$$

Specifically, $E_{xc}[\rho]$ has two components: an exchange functional, $E_x[\rho]$, and a correlation functional, $E_c[\rho]$.

$$E_{xc}[\rho] = E_x[\rho] + E_c[\rho] \quad \textbf{(2.8)}$$

$E_x[\rho]$ and $E_c[\rho$ functionals can be local as well as generalized-gradientfunctional.

Local density functionals(LDA) depend on electron density ρ, whereas generalized-gradient (GGA) functionals depend on both ρ and its gradient, Δρ.

A system of non-interacting electrons moving in an external effective potential v_{eff} (r) is shown as follows:

$$v_{eff}(r) = v(r) + \frac{\partial J[\rho]}{\partial \rho(r)} + \frac{\partial E_{xC}[\rho]}{\partial \rho(r)} = v(r) + \int \frac{\rho(r)}{|r-r'|} dr' + v_{xc}(r) \quad \textbf{(2.9)}$$

There is now an equation that is very similar to the Schrödinger equation.

$$\left[-\frac{1}{2}\nabla^2 + v_{eff}(r)\right]\psi_i = \varepsilon_i \psi_i \quad \textbf{(2.10)}$$

(2.4) to (2.9) are known as Kohn-Sham Equations.

The exchange-correlation functional is evaluated using several approximations. The first one is the local density approximation (LDA). The model is based on the concept of the uniform electron gas. The uniform electron gas model involves a large number of electrons uniformly spread out in a cube, where the positive charge is distributed uniformly to make the system neutral. The energy expression assumes that the charge density varies slowly throughout the molecule so that a localized region of the molecule behaves like a uniform electron gas.

$$E[\rho] = T_s[\rho] + \int \rho(r)v(r)\, dr + J[\rho] + E_{xc}[\rho] + E_b \quad \textbf{(2.11)}$$

In this equation, E_b is the electrostatic energy of the positive background. Since the positive charge density is negative to the electron density, the equation can be rewritten as follows:

$$E[\rho] = T_s[\rho] + E_{xc}[\rho] = T_s[\rho] + E_x[\rho] + E_c[\rho] \quad \textbf{(2.12)}$$

Exchange-functional may be defined in terms of electron density.

The DFT method involves the combination of an exchange functional and a correlation functional, thus defining LDA, GGA or hybrid functionals.

Unlike BLYP (Becke's gradient-corrected exchange functional combined with Lee-Yang-Parr's gradient-corrected correlation functional) B3LYP (Becke's three-

parameter functional combined with Lee-Yang-Parr correlation functional) is a hybrid functional combining LDA, B88, and LYP functionals.

$$Exc = E_{xc}^{LDA} + a_0(E_x^{exact} - E_x^{LDA}) + a_x\Delta E_x^{B88} + a_c\Delta E_c^{non-local} \quad \textbf{(2.13)}$$

It can then be shown that $\Delta E_x{}^{B88}$ is Becke's gradient correction and that Lee-Yang-Parr functional provides a correction for the correlation ($\Delta Ex_C{}^{non\text{-}local}$).

Becke specifies the parameters by fitting atomization energies, ionization potentials, proton affinities, and first row atomic energies in the molecule set, a0=0.20, ax=0.72 and ac=0.81. Compared to LDA and GGA functionals, hybrid functionals have been proven to be more effective (House, 2018).

2.1.1 Basis sets

A basis set consists of a set of mathematical functions. Slater type orbitals (STO) and gaussian type orbitals (GTO) are the frequently used basis functions which form the very well known STO-nG and split-valence basis sets. A number of basis sets are developed, such as the minimal basis sets (STO-3G), split-valence basis sets. (3-21G, 6-31G* , 6-31+G* ...) where (*) represents the polarization functions and (+) for diffuse functions.

In this study, both hybrid and dispersion corrected functionals were used. B3LYP which is a Becke three-parameter hybrid functional, LC-wPBE, and CAM-B3LYP which are functionals including long range correction (Sherrill, 2017).

2.1.2 The Basis set superposition error (BSSE)

The basis set superposition error (BSSE) is one of the major obstacles to the accurate prediction of interaction energies in quantum chemical calculations. There are several reasons why BSSE elimination is important, one of which is that the magnitude of the

BSSE can be large as compared to the interaction energy. BSSE is often cited as the source of overbinding of van der Waals complexes (Galano & Alvarez-Idaboy, 2006).

As described above, each monomer in the dimer can co-share basis functions from the other monomer, lowering the energy of the in order to compensate for BSSE, a variety of strategies can be applied. The counterpoise Method (CP) is commonly used method for eliminating BSSE. This method estimates the size of artificial stabilization. As a result of the CP method, the artificial energy provided by the orbitals of the monomers

to each other is added to the interaction energy to obtain the corrected energy value (Boys & Bernardi, 1970) . A and B are two fragments in equation 2.14.

$$E_{BSSE} = [E^{AB}(A) - E^{A}(A)] + [E^{AB}(B) - E^{B}(B)] \quad \textbf{(2.14)}$$

$$\Delta E_{int} = E^{AB}(AB) - E^{A}(A) - E^{B}(B) \quad \textbf{(2.15)}$$

$$\Delta E_{int}^{CP} = \Delta E_{int} + E_{BSSE} \quad \textbf{(2.16)}$$

3. METHODOLOGY

The gas phase geometry optimizations for dimer, trimer, tetramer, and pentamer oligomers of PNIPAAm, PEOVE, PNVIBA were performed by using Density Functional Theory (DFT). Calculations were carried out using the B3LYP functional and 6-31G(d,p) basis set, which are known to perform well when optimizing the geometry of organic molecules.. To obtain the global minimum structure on the potential surface of the molecule, many different conformers of the studied monomers were searched by performing a conformational analysis. Next, the electronic energies obtained from the optimization calculations were compared and the structures with the lowest energies were selected. In order to model hydrogen bond interactions, various configurations of water-pentamer complexes were studied. Water molecules were added in 1:1, 1:2, 1:3, 1:4 up to 1:18 ratios to the oligomeric chain of existing thermoresponsive oligomers, resulting in spatial configurations. Thermodynamically stable configurations were found after the geometry optimization. In order to provide a quantitative interpretation of the hydrogen bond, the interaction energies were calculated. The basis set superposition error (BSSE) was considered in all calculations. The zero point energy correction (ΔZPE) was also added to the interaction energies. Interaction energies were calculated with three types of functionals as B3LYP, LC-wPBE and CAM-B3LYP in 6-311G(2df,2pd) basis set.

As part of investigation, calculations were performed for monomer···monomer interactions with and without solvent molecules and the effect of the oligomer size on the conformations were studied. In order to observe conformational changes in the backbones, Radius of gyration (Rg) and Root-mean-square deviation (RMSD) were calculated between the oligomer-water complexes and the unhydrated oligomer chain.

All calculations in this study were executed by using the Gaussian '16 (Gaussian 09 Citation | Gaussian.Com, n.d.) software.

Throughout the thesis, the unit of the intermolecular distance (r_{int}) is given in Angstrom (Å) and the following color coding is utilized (Figure 3.1).

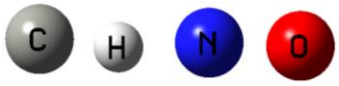

Figure 3.1: Color coding in GaussView

4. RESULT AND DISCUSSION

4.1 PNIPAAm

In order to observe the conformational transitions of a single chain, PNIPAAm was examined. To this end, the structure optimization of the dimer, trimer, tetramer, and pentamer oligomers of PNIPAAm(Figure 4.1) was performed in a vacuum by using density functional theory (DFT) with the B3LYP functional and 6-31G(d,p) basis set for their global minimum structures.

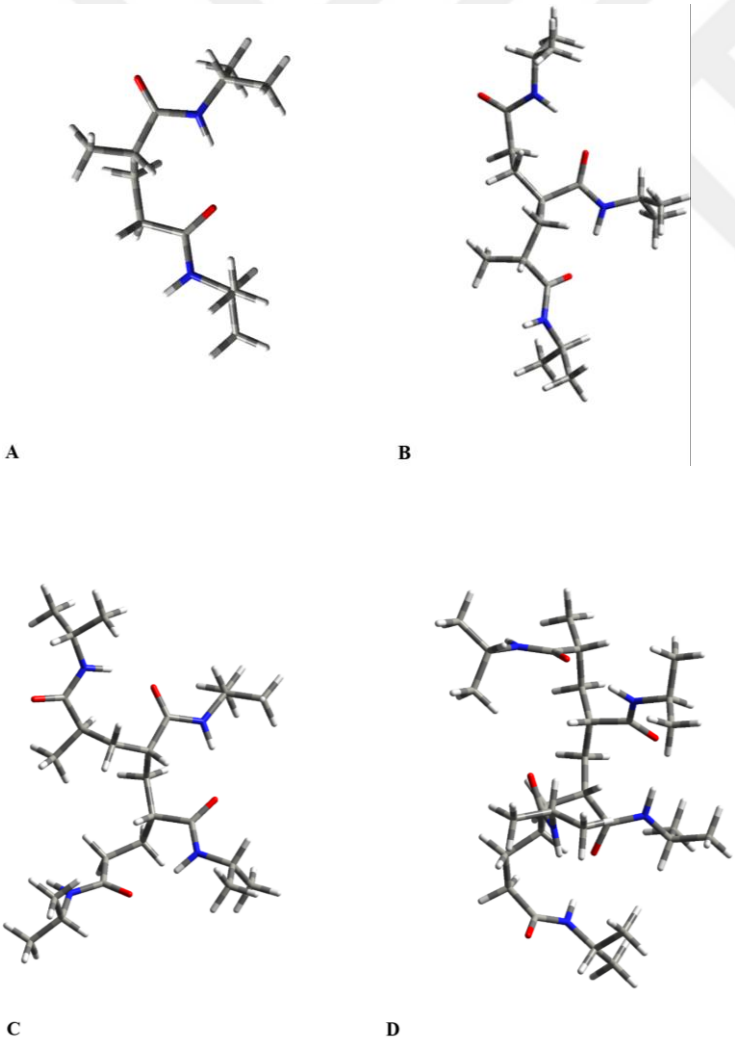

Figure 4.1: PNIPAAm (A) dimer (B) trimer (C) tetramer (D) pentamer

The pentamer,(Figure 4.1 D), the longest chain oligomer, was chosen to model PNIPAAm-water complexes. Figure 4.2, 4.3, 4.4, 4.5 illustrates the modeled PNIPAAm pentamer structures by adding water molecules at ratios of 1:1, 1:2, 1:3, 1:4, 1:5 to 1:18.

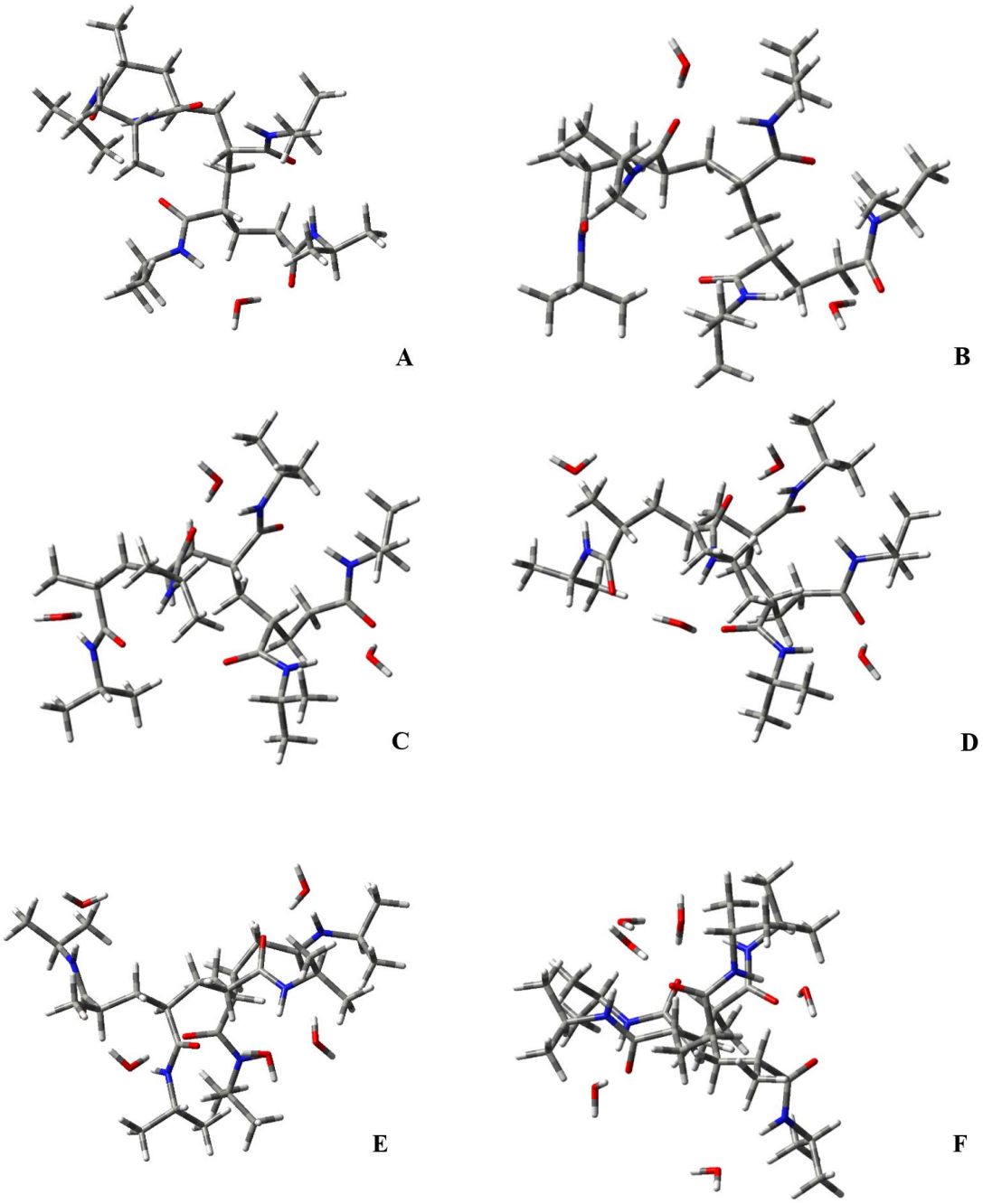

Figure 4.2: PNIPAAm pentamer /water systems with ratio of 1:1, 1:2, 1:3, 1:4,1:5 and 1:6 respectively.

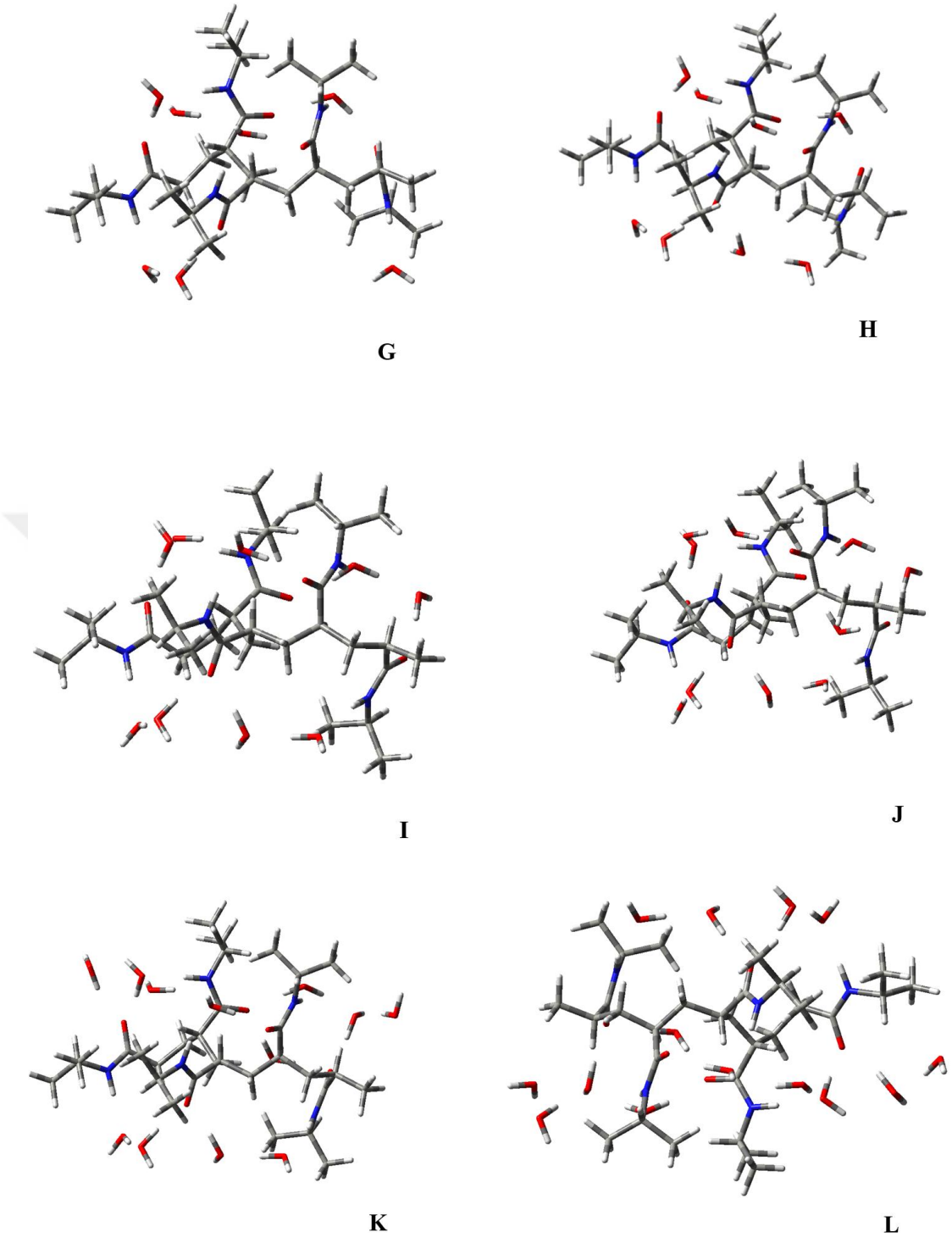

Figure 4.3: PNIPAAm pentamer /water systems with ratio of 1:7, 1:8, 1:9, 1:10, 1:12 and 1:14 respectively

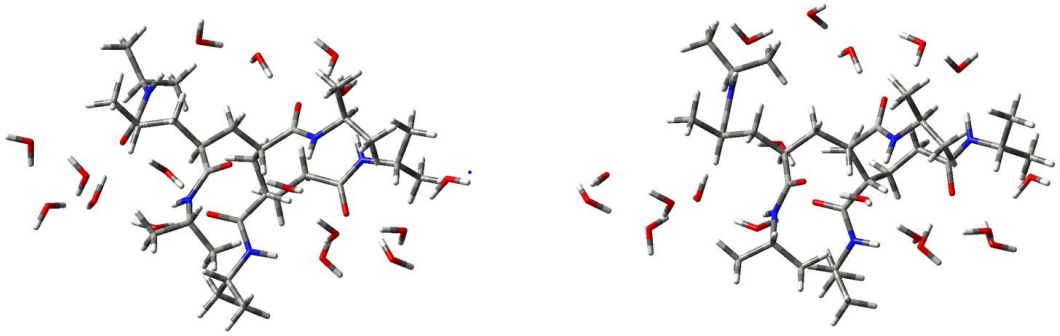

M **N**

Figure 4.4: PNIPAAm pentamer /water systems with ratio of 1:16, 1:18 respectively.

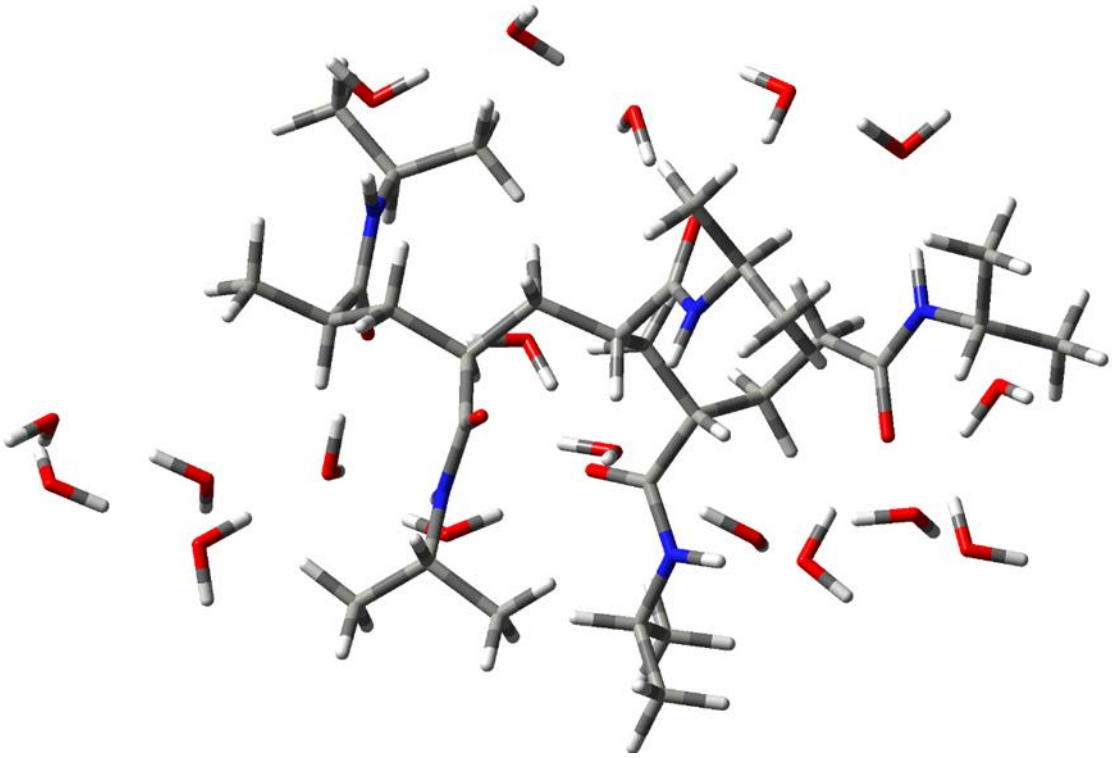

Figure 4.5: PNIPAAm pentamer /water systems with ratio of 1:18

The total interaction energy between PNIPAAm and water was calculated according to the following formula,

$$\mathrm{Eint} = \mathrm{Epw} - (\mathrm{E_P} + \mathrm{nE_w}) \qquad \textbf{(4.1)}$$

where E_P, E_W, and Epw are the energies of PNIPAAm pentamer, water molecules, and PNIPAAm-water complexes,respectively (n specifies the number of water molecules).

Interaction energies were also calculated with B3LYP, LC-wPBE, and CAM-B3LYP functionals and 6-311G(2df,2pd) basis set. The final results were additionally corrected by the basis set superposition error (BSSE) with counterpoise method.

Interaction energies were also corrected by the addition of zero point energies (ΔZPE). The results are summarized in Table 4.1

Table 4.1: The interaction energies of the optimized water-PNIPAAm complexes at different levels of theories in 6-311G(2df,2pd) basis [in kcal.mol^{-1}]

Composition (pentamer:water)	B3LYP	LC-wPBE	CAM-B3LYP	ZPE corrected
01:01	-11.97	-12.08	-13.92	-9.37
01:02	-18.16	-18.40	-21.47	-13.57
01:03	-22.26	-22.78	-26.61	-16.34
01:04	-40.22	-40.91	-47.39	-31.40
01:05	-56.46	-57.09	-66.05	-45.24
1:6	-65.34	-66.44	-76.93	-51.03
01:07	-73.06	-74.01	-85.64	-56.72
01:08	-78.17	-80.62	-93.62	-57.84
01:09	-85.56	-88.56	-102.69	-62.92
01:18	-222.02	-257.83	-280.73	

It is clear to conclude that increasing the number of water molecules resulted in stronger interactions. With the inclusion of fourth water molecule, it is observed that the geomery of the water molecules allowed more than one H-bonding interaction, thus, its contribution lowered the ineteraction energy values further.

Next, polymer segment···solvent and polymer segment···segment interactions were investigated to account on their impact on the polymer chain conformation in solutions. To demonstrate the interactions between polymer segments, monomer···monomer interactions of NiPAAm were considered. Monomer...monomer interaction energies were calculated at B3LYP/6-31G(d,p) level. (Figure 4.6)

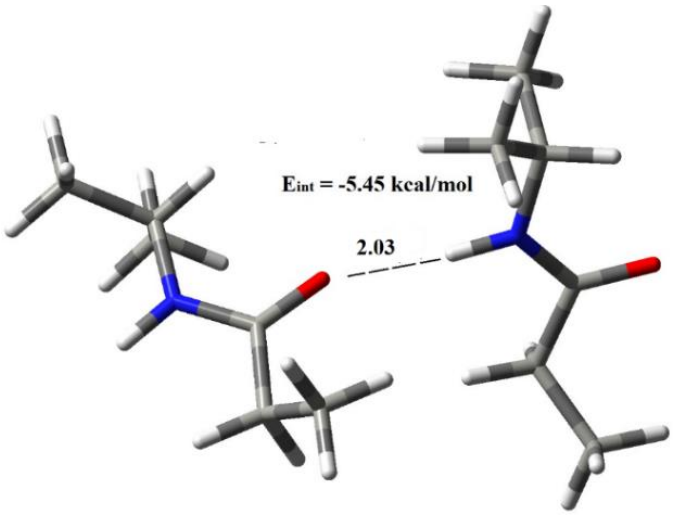

Figure 4.6: The structure and the corresponding interaction energy (E_{int}) of NiPAAm···NiPAAm monomers

The investigation also included calculations of the monomer-monomer interactions with solvents. (Figure 4.7)`

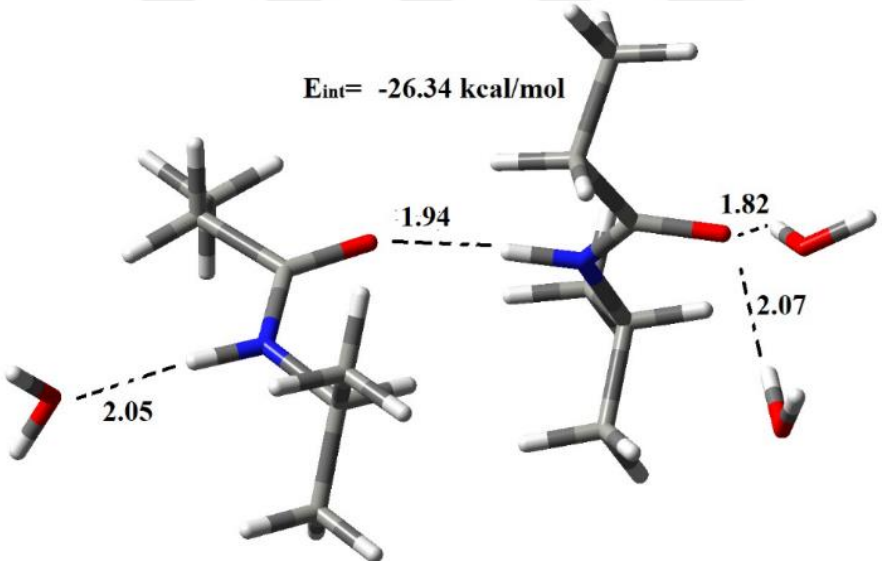

Figure 4.7: The structure and the interaction energy of NiPAAM···NiPAAM with 3 water moelcules

The structure and the interaction energy calculated by interacting NIPAAm with optimized two water molecules and NIPAAm with optimized one water molecule. Figure (4.8)

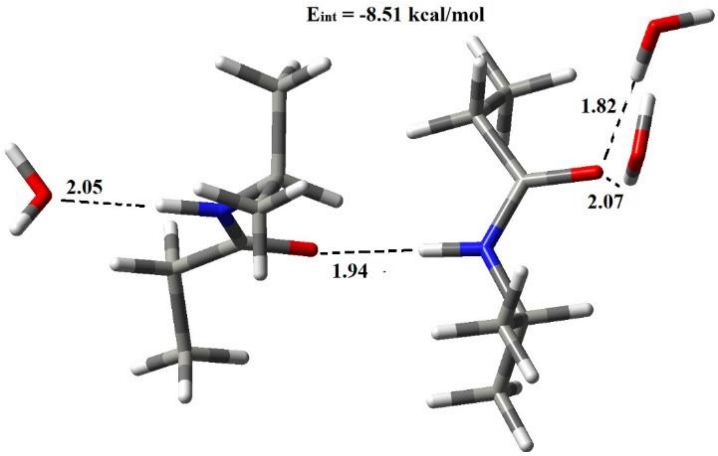

Figure 4.8: The interaction energy of NIPAAm(2w)…NIPAAm(1w)

Dimer ···dimer interactions with and without solvents are considered to observe the effect of the oligomer size on the single chain.(Figure 4.9 and 4.10)

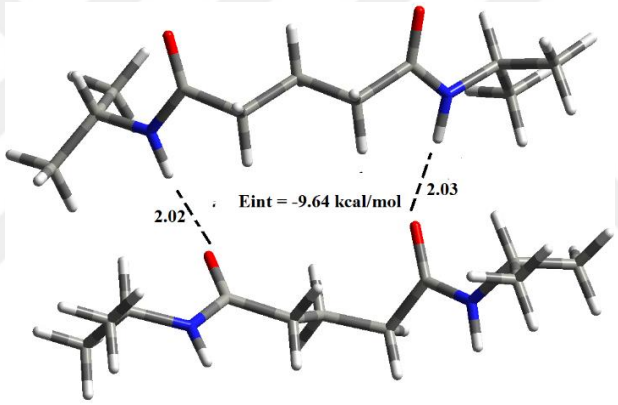

Figure 4.9: The interaction energy of dimer NIPAAm…dimer NIPAAm

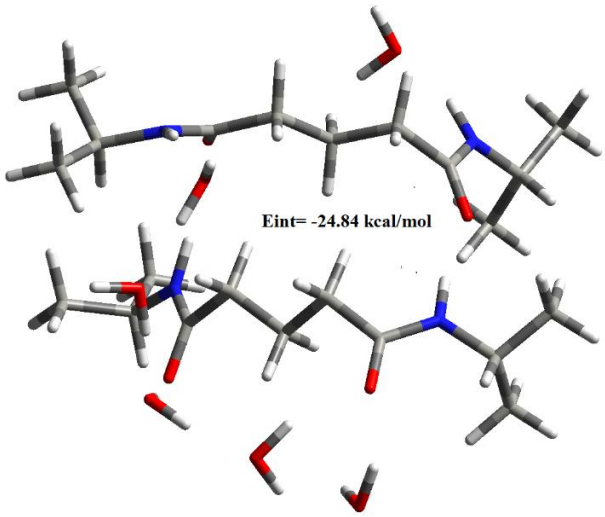

Figure 4.10: The interaction energy of dimer NIPAAm… dimer NIPAAm with solvent

Comparison of the interaction energy values of dimer and monomer NIPAm..NIPAm were listed in Table 4.2.

Table 4.2: Comparison of the interaction energy of dimer and monomer

E_{int} monomer..monomer (kcal/mol)	E_{int} dimer....dimer (kcal/mol)
-5.45	-9.64
E_{int} monomer..monomer with water	E_{int} dimer....dimer with water
-8.51	-24.84

The results have shown us that increasing the length of the single chain without water results with a lower interaction energy of -9.64 kcal/mol as compared to -5.45 kcal/mol for the monomer. As a result of the presence of water molecules in the dimer oligomer environment, it exhibits a stronger impact and decreases the interaction enery even further to -24.84 kcal/mol, as compared to -8.51 kcal/mol for the monomer. In the presence of water molecules, the total interaction becomes stronger and also the effect of water media on the strength of the interaction is more clear in the dimeric structure compared to the monomer case.

Listed Table 4.3 presents the calculated values and their comparison to those in the study of Juan Pang et al. (Pang et al., 2011)

Table 4.3: Comparison of the calculated energies from this work and from literature.

	this work B3LYP/6-31G(d,p)	Ref* MP2/6-31G+G(d,p)
Monomer /monomer	-5.45	-5.43
2Monomer / 3W	-26.34	-
Monomer+1W / monomer +2W	-8.51	-8.25

*. Pang et al., 2011

As a further investigation, Pymol (PyMOL | Pymol.Org, n.d.) was used to calculate the Root-mean-square deviation (Rmsd) value. The value of the Rmsd was found 0.247 Å. The backbones of PNIPAAm pentamer and PNIPAAm-18 water complex are overlapped to observe the conformational changes. (Figure 4.11)

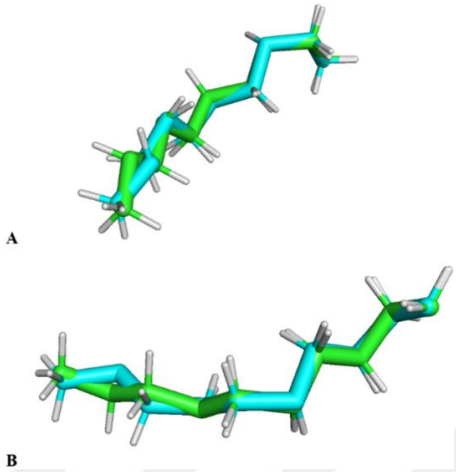

Figure 4.11: (A,B) Images of the overlap of PNIPAAm pentamer (green) and PNIPAAm-18 water complex (blue) backbones from different angles**)**

Radius of gyration (Rg) of the single chain represents the size and conformation of the oligomer during the simulation; larger Rg values indicate extended states, while smaller Rg values indicate collapsed states. Therefore, radius of gyration value was also calculated for further investigation on the change of the chain conformation. The results are summarized in Table 4.4.

Table 4.4: Radius of gyration values for PNIPAAm

	Radius of gyration values (Å)
PNIPAAm /18 water complex	5.14
PNIPAAm pentamer	6.31

The radius of gyration value of PNIPAAm -18 water complex is lower than pentamer without water. These results demonstrate that the chain ends are getting closer to one another, that is, the Rg value indicates the transition from extended states to collapsed state. De Oliveira et al. have studied simulations of single-chain oligomers of PNnPAm from 4 to 32-mers to understand the changes in the radius of gyration induced by the coil-toglobule transition of PNnPAm below and above the LCST. It has been found that Rg is equal to 6.6 Å for oligomers with 8-mers. (de Oliveira et al., 2018)

4.2 PNVIBA

Figure 4.12 ilustrates the optimized structure of PNVIBA pentamer.

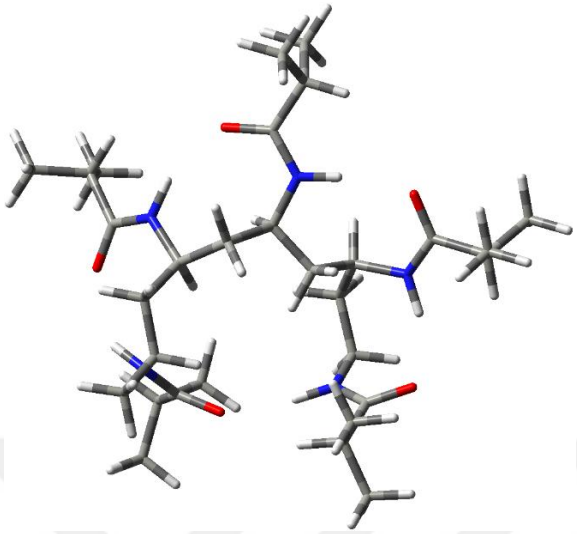

Figure 4.12: PNVIBA pentamer

Figures 4.13, 4.14, 4.15, 4.16 illustrates PNVIBA pentamer modeled structures by adding water molecules at ratios of 1:1, 1:2, 1:3, 1:4, 1:5 to 1:18.

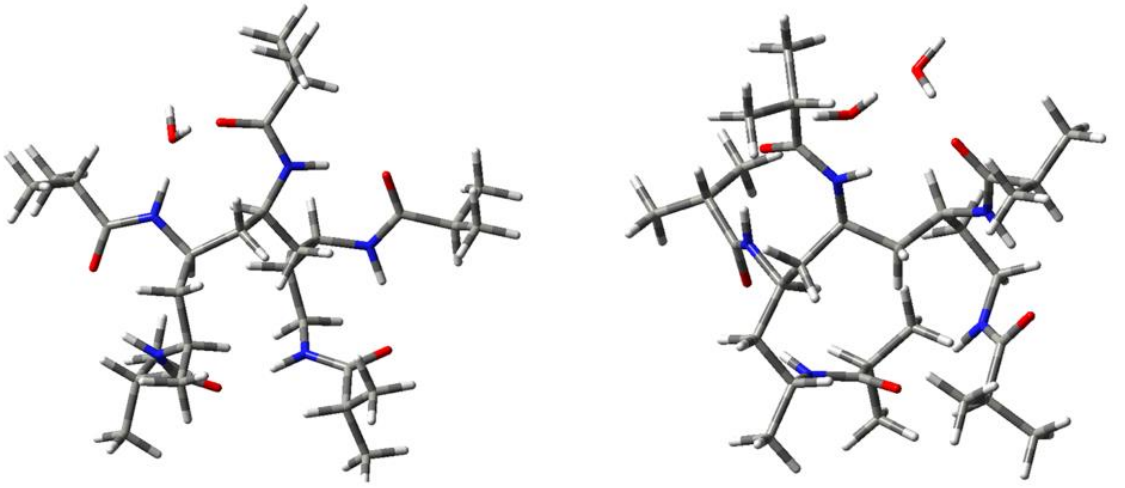

Figure 4.13: PNVIBA pentamer /water systems with ratio of 1:1, 1:2 respectively

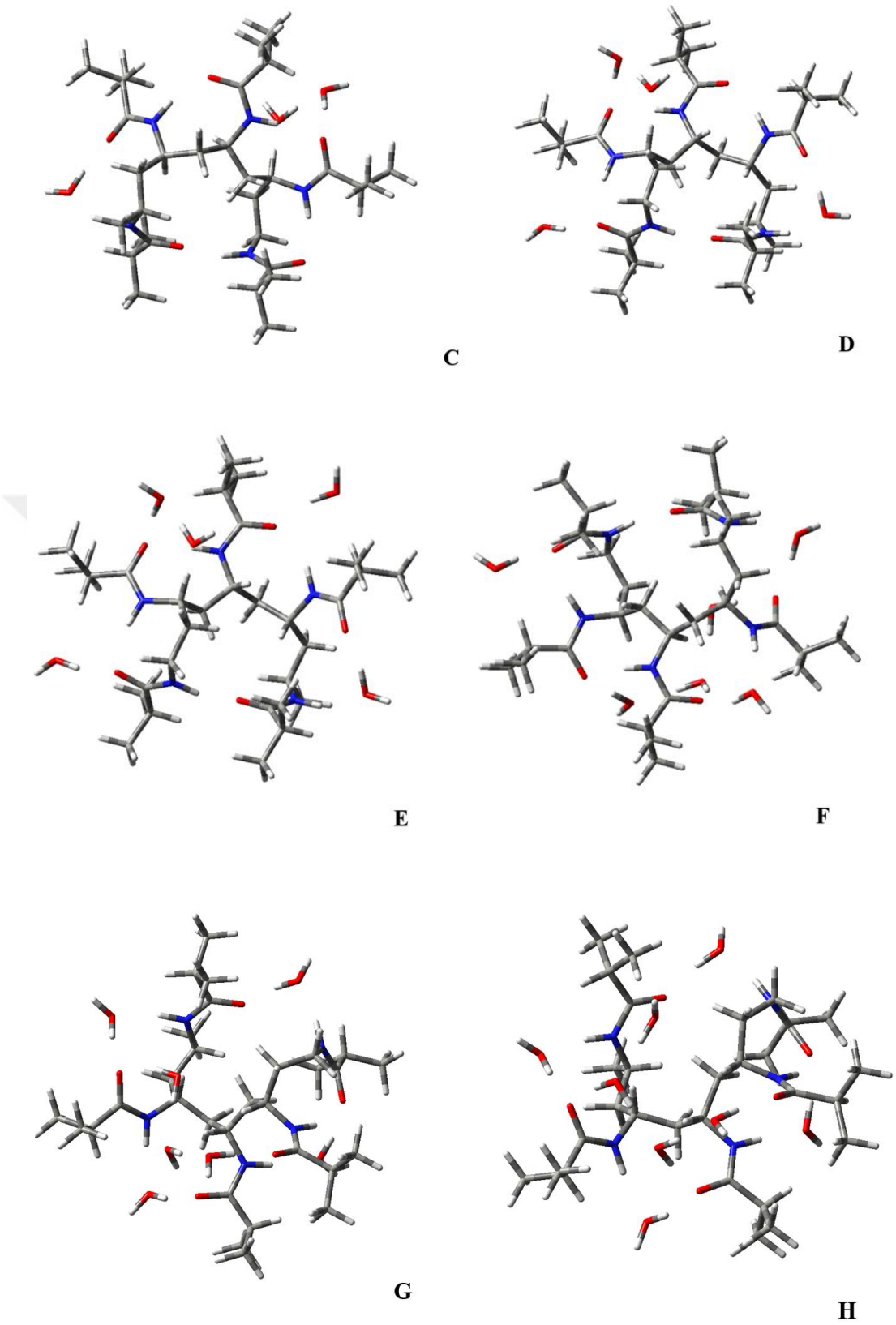

Figure 4.14: PNVIBA pentamer /water systems with ratio of 1:3, 1:4, 1:5, 1:6,1:7 and 1:8 respectively

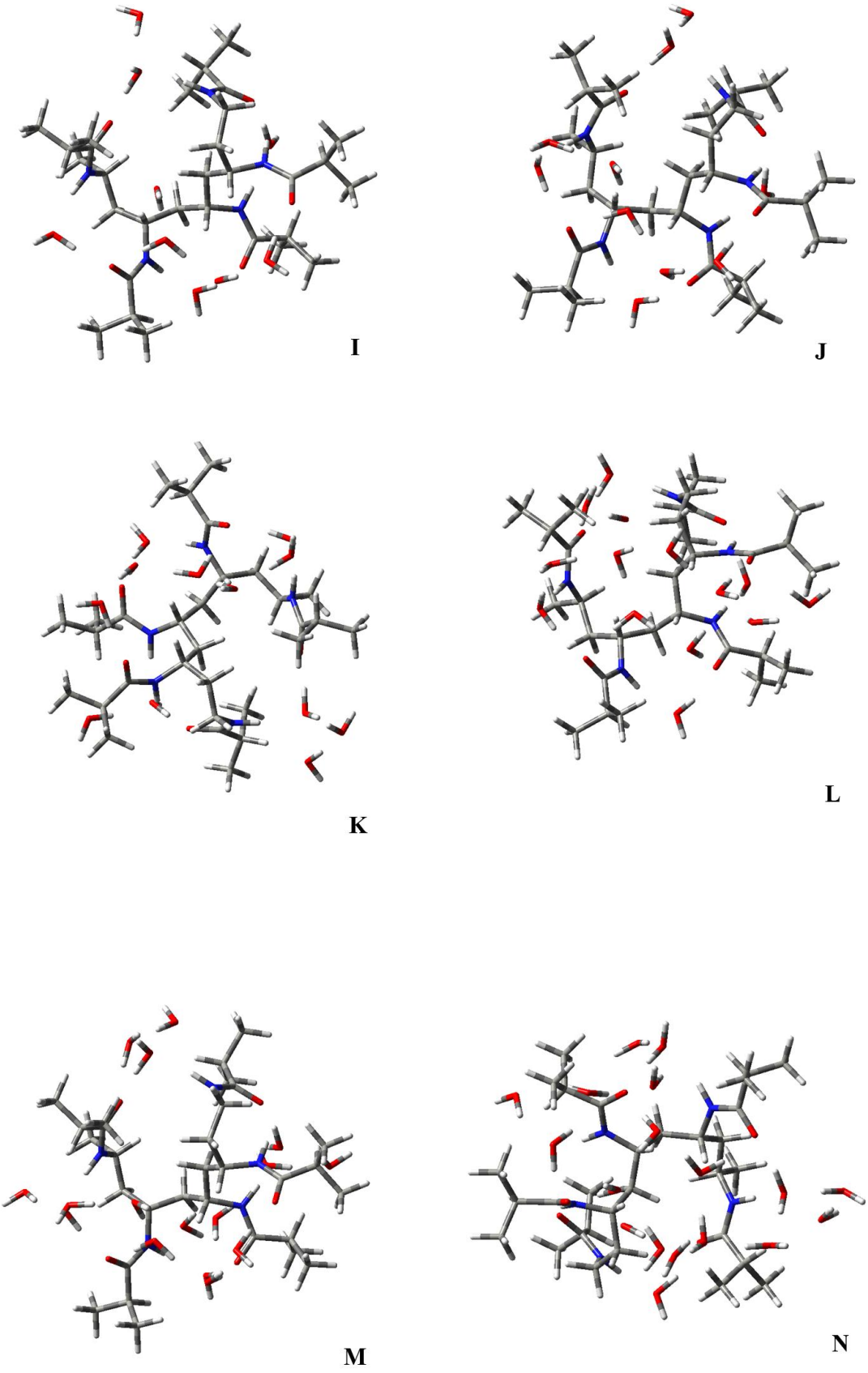

Figure 4.15: PNVIBA pentamer /water systems with ratio of 1:9, 1:10, 1:12, 1:14, 1:16 and 1:18 respectively

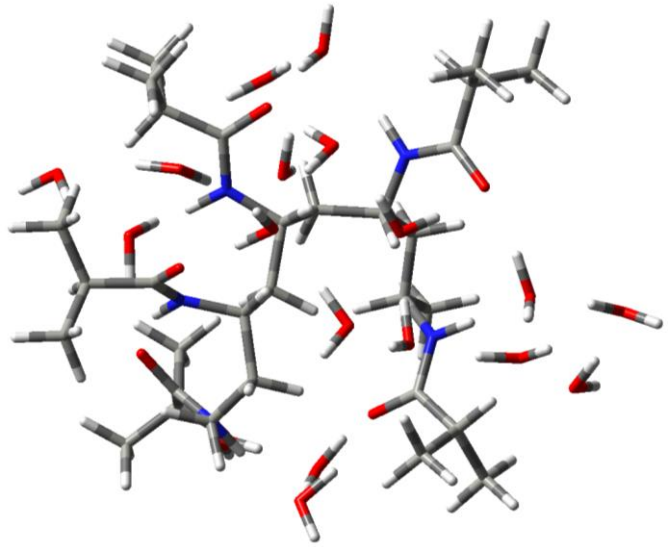

Figure 4.16: The structure of PNVIBA with 18 water molecules

PNVIBA-water interaction energy was calculated using the equation 4.1. In all of the investigated systems, geometry optimizations were performed for PNVIBA pentamer, water molecules, and PNVIBA-water complexes and basis set superposition error (BSSE) was additionally applied to correct the final result. Additionally, zero point energy (ΔZPE) was also added to the interaction energies to correct them. The results are summarized in Table 4.5.

Interaction energies were also calculated with B3LYP, LC-wPBE, and CAM-B3LYP functionals and 6-311G(2df,2pd) basis set.

Table 4.5: The interaction energies of the optimized water-PNVIBA complexes at different levels of theories in 6-311G(2df,2pd) basis [in kcal.mol-1]

Composition pentamer:water	B3LYP	LC-wPBE	CAM-B3LYP	ZPE corrected
1:1	-5.75	-6.03	-7.23	-3.84
1:2	-14.85	-15.80	-18.39	-10.39
1:3	-26.35	-26.60	-30.95	-19.88
1:4	-32,83	-29.24	-35.11	-24.30
1:5	-38.20	-38.73	-45.63	-27.87
1:18	-169.11	-172.03	-199.18	-123.2

The energy of each hydrogen bond is approximately equal to -5 kcal/mol. It is clear to conclude that the addition of a second water molecule allowed more than one H-

bonding interaction, thus, its contribution lowered the ineteraction energy values further. Thus, the total interaction becomes stronger.

NVIBA…NVIBA monomer-monomer interactions were shown in Figure 4.17.

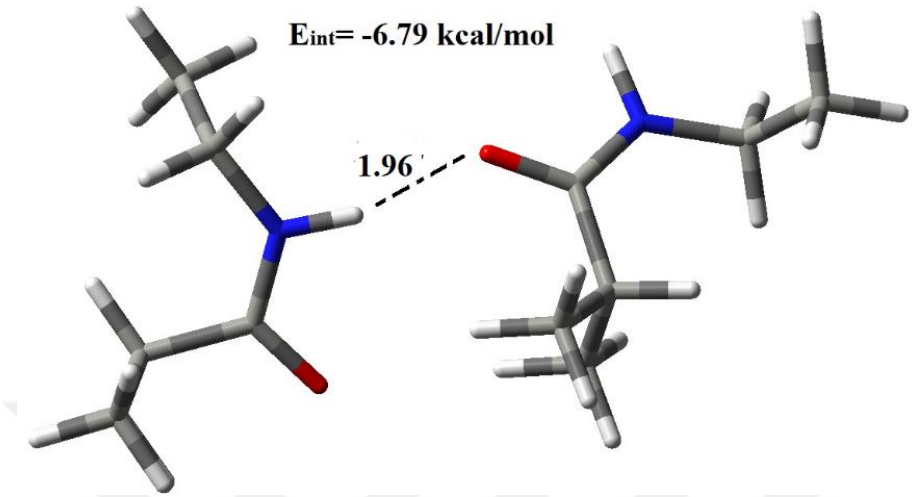

Figure 4.17: Optimized structure and the interaction energy (E_{int}) at B3LYP/6-31G(d,p) level for NVIBA…NVIBA monomer-monomer interaction.

NVIBA…NVIBA monomer-monomer interactions with solvents were shown in Figure 4.18 and 4.19.

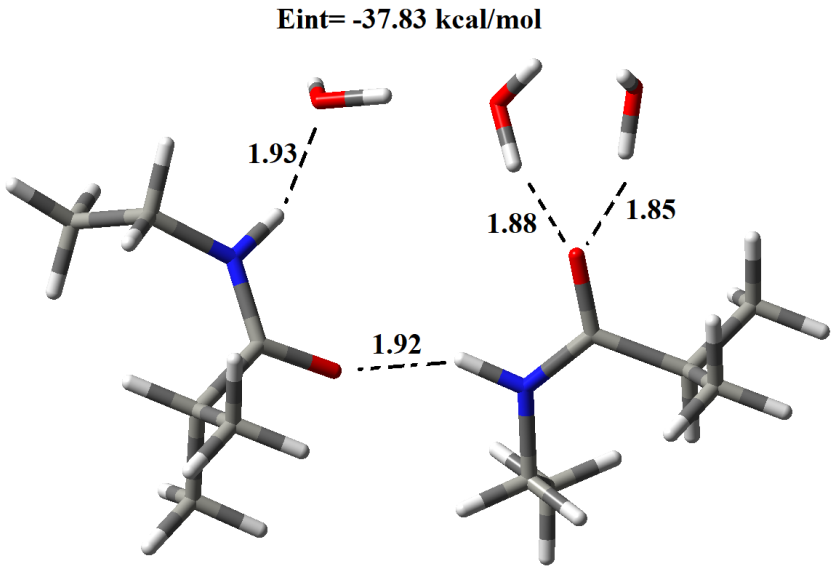

Figure 4.18: Optimized structure and the interaction energy (E_{int}) of NVIBA-NVIBA monomer interaction with 3 water molecules calculated at B3LYP/6-31G(d,p) level of theory.

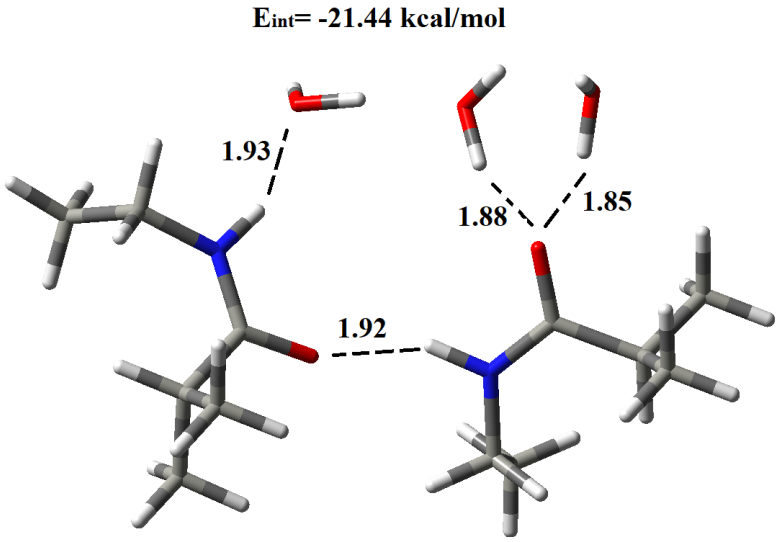

Figure 4.19: Optimized structure and the interaction energy (E_{int}) of NVIBA(2w)…NVIBA(1w) fragments calculated at B3LYP/6-31G(d,p) level of theory.

It is clear to conclude that monomer with water molecules present in the segments formed stronger interactions, as expected.

RMSD value was found 0.646 Å by using PyMOL programme (PyMOL | Pymol.Org, n.d.). The backbones of PNVIBA pentamer and PNVIBA-18 water complex are overlapped to observe the conformational changes. (Figure 4.20)

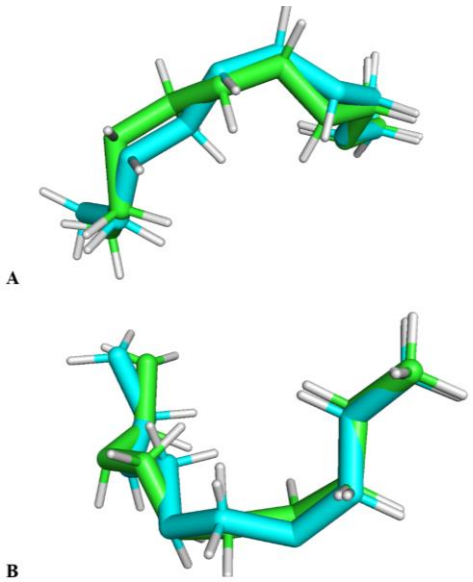

Figure 4.20: (A,B) Images of the overlap of PNVIBA pentamer (green) and PNVIBA-water complex (blue) backbones from different angles

The results of the radius of gyration values(Rg) are summarized in Table 4.6

Table 4.6: Radius of gyration values for PNVIBA

	Radius of gyration values (Å)
PNVIBA/18 water complexes	6.31
PNVIBA pentamer	7.24

The difference in radius of gyration between pentamer without water and PNVIBA -18 water complex is 0.93 Å. The radius of gyration value of PNVIBA -18 water complex is lower than pentamer without water. This indicates the transition from an extended state to a collapsed state.

4.3 PEOVE

In the final part of the investigation, PEOVE was examined in order to observe conformational transitions within a single chain.The optimized structure of PEOVE pentamer was shown in Figure 4.21

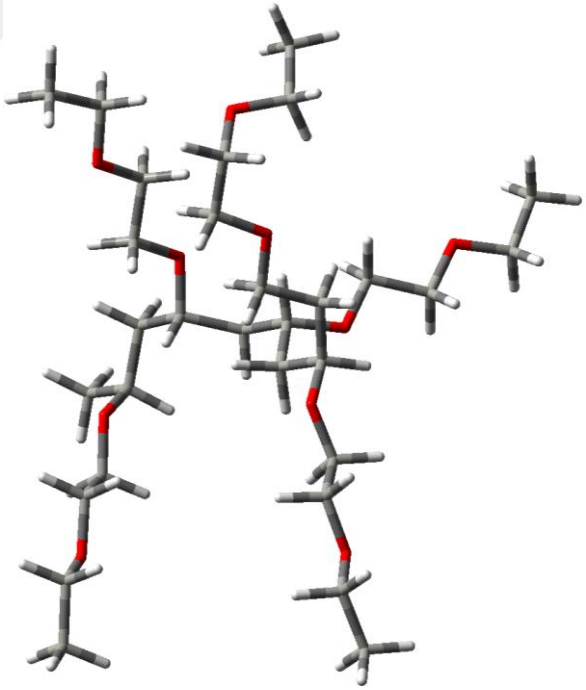

Figure 4.21: The optimized structure of PEOVE pentamer

Figures 4.22, 4.23, 4.24, 4.25 illustrates PEOVE pentamer modeled structures by adding water molecules at ratios of 1:1, 1:2, 1:3, 1:4, 1:5 up to 1:18.

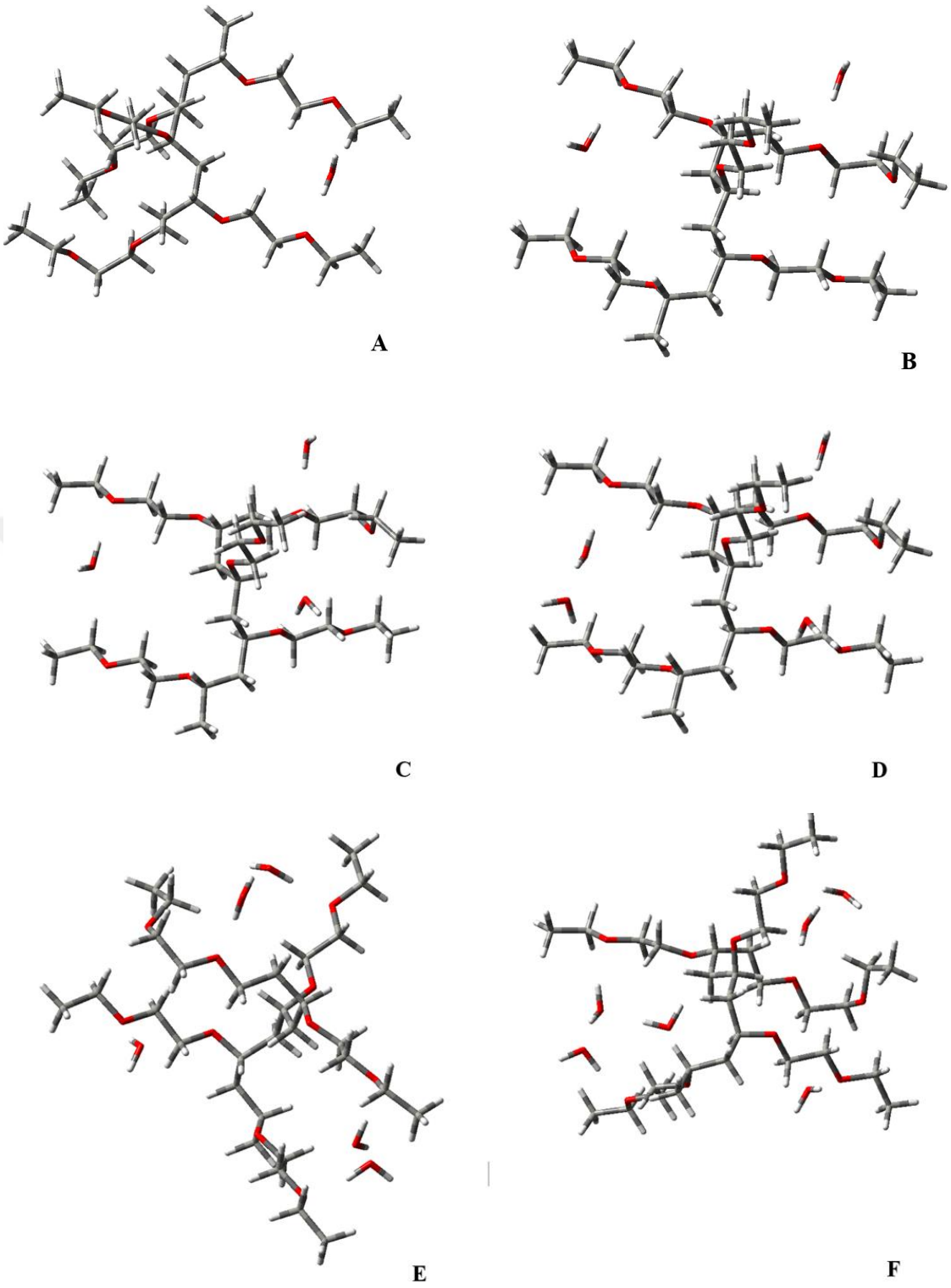

Figure 4.22: PEOVE pentamer /water systems with ratio of 1:1, 1:2, 1:3, 1:4, 1:5 and 1:6 respectively

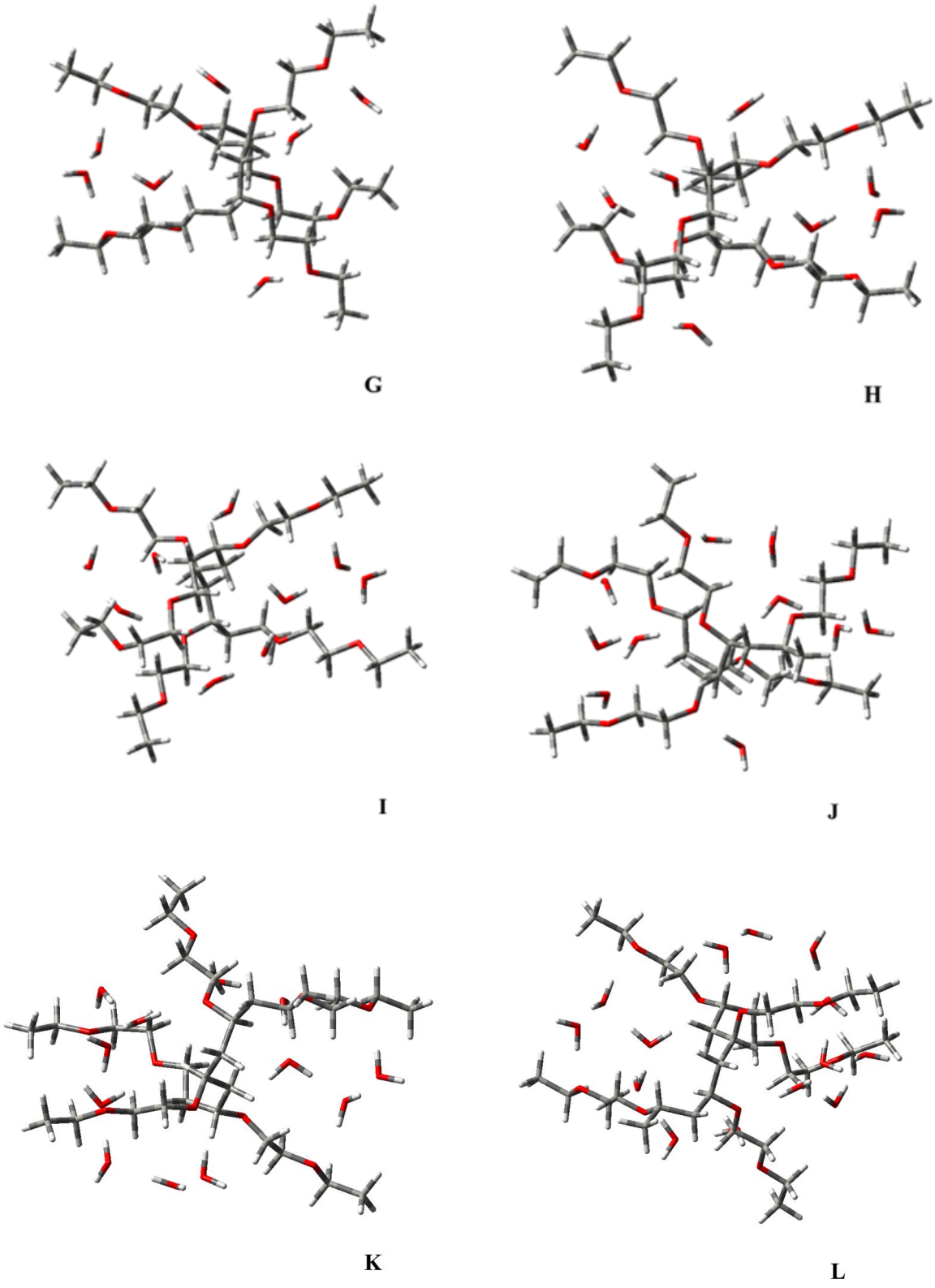

Figure 4.23: PEOVE pentamer /water systems with ratio of 1:7 , 1:8, 1:9, 1:10, 1:12, 1:14 respectively

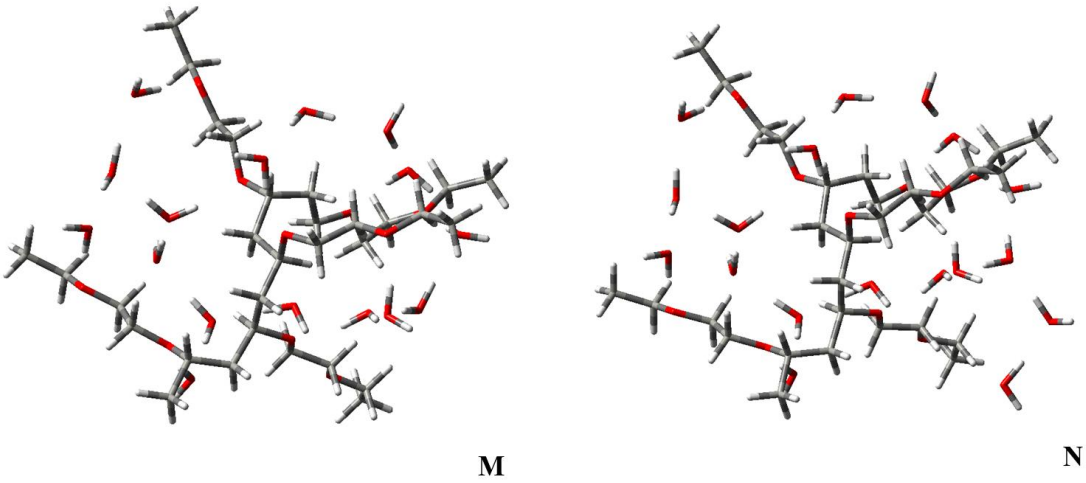

Figure 4.24: PEOVE pentamer /water systems with ratio of 1:16, 1:18, respectively

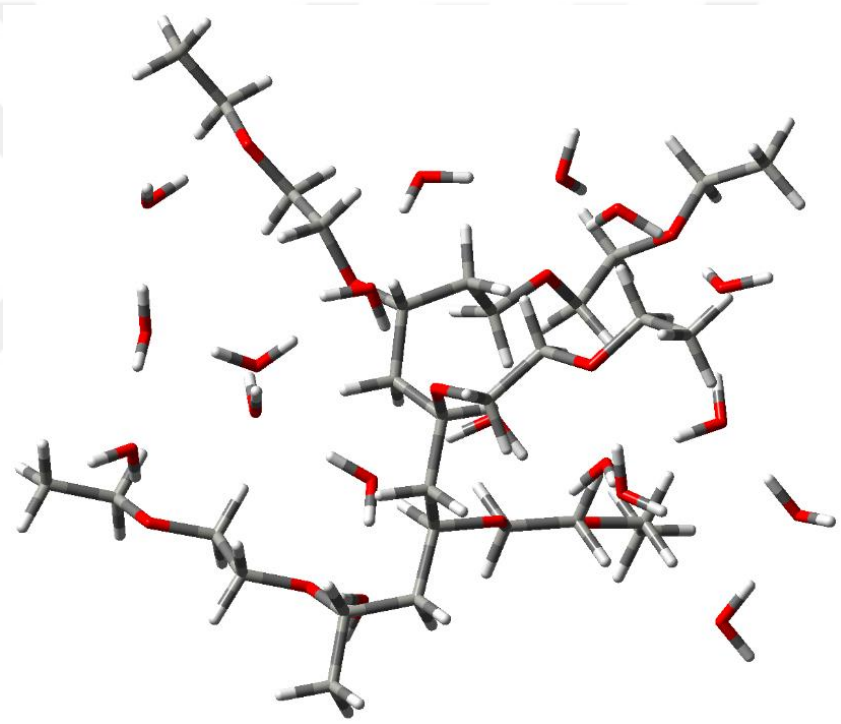

Figure 4.25: The structure of PEOVE with 18 water

PEOVE-water interaction energy was calculated using the equation 4.1. The results are summarized in Table 4.7.

Table 4.7: The interaction energies of the studied PEOVE-water complexes at different levels of theories with the 6-311G(2df,2pd) basis set [in kcal.mol-1]

Composition (pentamer:water)	B3LYP	LC-wPBE	CAM-B3LYP	ZPE corrected
01:01	-5.22	-5.58	-6.76	-2.94
01:02	-9.37	-10.16	-12.12	-5.08
01:03	-14.95	-16.15	-19.33	-8.45
01:04	-23.85	-25.31	-30.14	-14.14
01:05	-28.26	-30.11	-35.75	-16.51
01:18	-214.83	-248.33	-271.54	

The energy of a hydrogen bond is approximately equal to -5. kcal/mol, and total interaction increases with each hydrogen bond added to the structure. It is clear to conclude that the addition of fourth water molecule makes two more hydrogen bonds, as in PEOVE case.

RMSD value was found as 0.078 Å by using PyMOL programme (PyMOL | Pymol.Org, n.d.). The backbones of PEOVE pentamer and the PEOVE-18 water complex are overlapped to observe the conformational changes. (Figure 4.26)

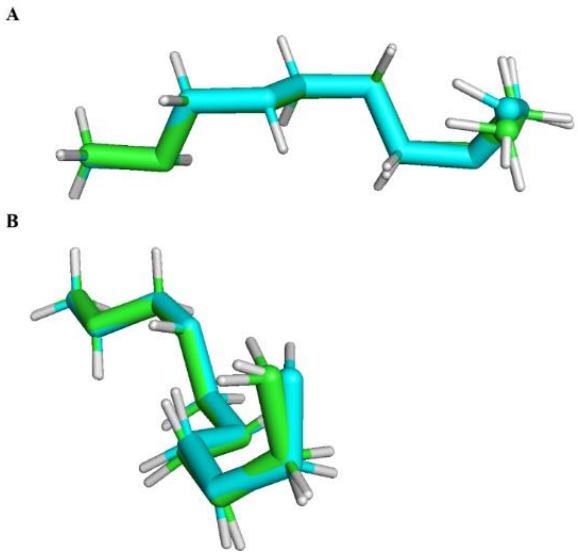

Figure 4.26: Images of the overlap of PEOVE pentamer (green) and PEOVE-18 water complex (blue) backbones from different angles

The results of the radius of gyration values(Rg) are summarized in Table 4.8

Table 4.8 Radius of gyration values for PEOVE

	Radius of gyration values (Å)
PEOVE/18 water complexes	8.46
PEOVE pentamer	9.14

The difference in radius of gyration between pentamer without water and PEOVE -18 water complex is 0.68 Å. The radius of gyration value of PEOVE -18 water complex is lower than pentamer without water. This indicates the transition from an extended state to a collapsed state.

5. CONCLUSION

The thermo-responsive behavior of polymers in solution is determined by the hydrophobic and hydrogen bonding interactions between the polymer segments and the solvent. These thermo-responsive polymers exhibit a significant chain conformation change in the presence of water molecules at transition temperatures. The understanding of conformational transitions in polymer chains is crucial to understand the role played by the functional groups and how they interact with water. For this reason, in this thesis, an investigation was performed to understand the effect of the intermolecular interactions on conformational transitions of temperature-responsive materials that exhibit LCST behavior in water using quantum mechanical methods. To this end, Poly (N-isopropylacrylamide) (PNIPAAm), Poly(N-vinylisobutyramide) (PNVIBA), and poly(2-ethoxyethyl vinyl ether)(PEOVE) exhibiting LCST behavior in water were studied to examine structural changes by using DFT. In order to model the hydrogen bond interaction between the water molecule and the pentamer chain, which is the longest oligomer chain optimized, the water molecule was incorporated into the oligomer chain in ratios up to 1:18. The interaction energies of PNIPAm, PNVBA, and PEOVE were calculated by considering basis set superposition error (BSSE) and ZPE corrections. As a result of our calculations, the increasing number of water molecules results in an increase in the strength of the interaction.(Table 4.1, Table 4.5, Table 4.7)

Two kinds of molecular interactions are thought to be principally responsible for the conformational status of macromolecules in solution: polymer segment···solvent and polymer segment···segment interactions. It is clear to conclude that the competition between these two types of interactions results in different conformations of polymer chains in solutions. With this aim, monomer···monomer interactions with and without solvents and the effect of the oligomer size on the conformations were investigated.

In consequence, in the presence of water molecules, the total interaction becomes stronger and also the effect of water media on the strength of the interaction is more clear in the dimeric structure compared to the monomer case. (Figure 4.10)

In order to observe conformational changes in the backbones, Radius of gyration (Rg) and Root-mean-square deviation (RMSD) were calculated between the oligomer-18 water complexes and the unhydrated oligomer chains. Based on the results, it can be concluded that the chain ends are getting closer to one another, in other words, the Rg value indicates the transition from extended states to collapsed states.(Table 4.4, Table 4.6, Table 4.8)

According to literature, the difference of radius of gyration (Rg) values of a PnnPAm has been found 1 Å despite of length of chain N = 32 mer by using molecular dynamics.With this work herein, we showed that at least two oligomeric chains are required to consider intramolecular and intermolecular interactions. Therefore, it is possible to observe a significant change (de Oliveira et al., 2018).

REFERENCES

Abbott, L. J., & Stevens, M. J. (2015). A temperature-dependent coarse-grained model for the thermoresponsive polymer poly(N -isopropylacrylamide). *Journal of Chemical Physics*, *143*(24). https://doi.org/10.1063/1.4938100

Aguilar, M. R., & San Román, J. (2019). Introduction to Smart Polymers and Their Applications. In *Smart Polymers and their Applications* (pp. 1–11). Elsevier. https://doi.org/10.1016/b978-0-08-102416-4.00001-6

Alaghemandi, M., & Spohr, E. (2013). A molecular dynamics study of poly(N-isopropylacrylamide) endgrafted on a model cylindrical pore surface. *RSC Advances*, *3*(11), 3638–3647. https://doi.org/10.1039/c3ra22266g

Aoshima, S., D A, H. O., & Kobayashi, E. (n.d.). *Synthesis of Thermally-Induced Phase Separating Polymer with Well-Defined Polymer Structure by Living Cationic Polymerization. I. Synthesis of Poly (vinyl Ether)s with Oxyethylene Units in the Pendant and Its Phase Separation Behavior in Aqueous Solution*.

Azmi, N. S., Kamaruddin, N. N., Kassim, S., & Harun, N. A. (2018). Synthesis and characterization of hydrophilic polymer nanoparticles using n-isopropylacrylamide (NIPAM) via emulsion polymerization technique. *IOP Conference Series: Materials Science and Engineering*, *440*(1). https://doi.org/10.1088/1757-899X/440/1/012008

Birshtein, T. M., & Buldyrev, S. v. (1991). *Universality of properties of coil-globule transitions in different two-dimensional lattice models of a macromolecule*.

Boys, S. F., & Bernardi, F. (1970). The calculation of small molecular interactions by the differences of separate total energies. Some procedures with reduced errors. *Molecular Physics*, *19*(4), 553–566. https://doi.org/10.1080/00268977000101561

de Oliveira, T. E., Marques, C. M., & Netz, P. A. (2018). Molecular dynamics study of the LCST transition in aqueous poly(: N-n-propylacrylamide). *Physical Chemistry Chemical Physics*, *20*(15), 10100–10107. https://doi.org/10.1039/c8cp00481a

Deshmukh, S. A., Kamath, G., Mancini, D. C., Sankaranarayanan, S. K. R. S., & Jiang, W. (2014). Meso-scale Simulations of Poly(N-isopropylacrylamide) Grafted Architectures. *MRS Proceedings*, *1619*. https://doi.org/10.1557/opl.2014.542

Deshmukh, S. A., Sankaranarayanan, S. K. R. S., Suthar, K., & Mancini, D. C. (2012). Role of solvation dynamics and local ordering of water in inducing conformational transitions in poly(N -isopropylacrylamide) oligomers through the LCST. *Journal of Physical Chemistry B*, *116*(9), 2651–2663. https://doi.org/10.1021/jp210788u

Deshmukh, S., Mooney, D. A., McDermott, T., Kulkarni, S., & Don MacElroy, J. M. (2009). Molecular modeling of thermo-responsive hydrogels: Observation of lower critical solution temperature. *Soft Matter*, *5*(7), 1514–1521. https://doi.org/10.1039/b816443f

Encyclopedia of Polymeric Nanomaterials. (2015). In *Encyclopedia of Polymeric Nanomaterials*. Springer Berlin Heidelberg. https://doi.org/10.1007/978-3-642-29648-2

Flemming, P., Münch, A. S., Fery, A., & Uhlmann, P. (2021). Constrained thermoresponsive polymers - new insights into fundamentals and applications. In *Beilstein Journal of Organic Chemistry* (Vol. 17, pp. 2123–2163). Beilstein-Institut Zur Forderung der Chemischen Wissenschaften. https://doi.org/10.3762/bjoc.17.138

Galano, A., & Alvarez-Idaboy, J. R. (2006). A new approach to counterpoise correction to BSSE. *Journal of Computational Chemistry*, *27*(11), 1203–1210. https://doi.org/10.1002/jcc.20438

Gaussian 09 Citation | *Gaussian.com*. (n.d.). Retrieved December 14, 2022, from https://gaussian.com/g09citation/

Ghizal, R., Roohi, G., & Srivastava, F. S. (2014). Smart Polymers and Their Applications. In *International Journal of Engineering Technology* (Vol. 2, Issue 4). www.ijetmas.com

Gobeze, H. B., Ma, J., Leonik, F. M., & Kuroda, D. G. (2020). Bottom-up approach to assess the molecular structure of aqueous poly(N-isopropylacrylamide) at room temperature via infrared spectroscopy. *Journal of Physical Chemistry B*, *124*(51), 11699–11710. https://doi.org/10.1021/acs.jpcb.0c08424

Grabowski, S. J. (2004). Hydrogen bonding strength - Measures based on geometric and topological parameters. In *Journal of Physical Organic Chemistry* (Vol. 17, Issue 1, pp. 18–31). https://doi.org/10.1002/poc.685

House, J. E. (2018). Comments on Computational Methods. In *Fundamentals of Quantum Mechanics* (pp. 335–347). Elsevier. https://doi.org/10.1016/b978-0-12-809242-2.00014-0

Imberg, A. (n.d.). *On phase behaviours in liquid/polymer/solvent/water systems and their application for formation of lipid/polymer composite particles*.

James, H., John, R., Alex, A., B, K. A.-A. P. S., & 2014, undefined. (n.d.). Smart polymers for the controlled delivery of drugs–a concise overview. *Elsevier*. Retrieved August 2, 2022, from https://www.sciencedirect.com/science/article/pii/S2211383514000252

Jeffrey, G. A. (1996). Hydrogen bonds and molecular recognition. In *Food Chemistry* (Vol. 56, Issue 3).

Kamath, G., Deshmukh, S. A., Baker, G. A., Mancini, D. C., & Sankaranarayanan, S. K. R. S. (2013). Thermodynamic considerations for solubility and conformational transitions of poly-N-isopropyl-acrylamide. *Physical Chemistry Chemical Physics*, *15*(30), 12667–12673. https://doi.org/10.1039/c3cp44076a

Katsumoto, Y., Tanaka, T., Sato, H., & Ozaki, Y. (2002). Conformational change of poly(N-isopropylacrylamide) during the coil-globule transition investigated by attenuated total reflection/infrared spectroscopy and density functional theory calculation. *Journal of Physical Chemistry A*, *106*(14), 3429–3435. https://doi.org/10.1021/jp0124903

Kuckling, D., Adler, H.-J. P., Arndt, K.-F., Ling, L., & Habicher, W. D. (2000). Temperature and pH dependent solubility of novel poly(N-isopropylacrylamide) copolymers. In *Macromol. Chem. Phys* (Vol. 201).

Kuckling, D., Doering, A., Krahl, F., & Arndt, K. F. (2012). Stimuli-Responsive Polymer Systems. In *Polymer Science: A Comprehensive Reference, 10 Volume Set* (Vol. 8, pp. 377–413). Elsevier. https://doi.org/10.1016/B978-0-444-53349-4.00214-4

Kumar, A., Srivastava, A., Galaev, I. Y., & Mattiasson, B. (2007). Smart polymers: Physical forms and bioengineering applications. In *Progress in Polymer Science (Oxford)* (Vol. 32, Issue 10, pp. 1205–1237). https://doi.org/10.1016/j.progpolymsci.2007.05.003

Lanzalaco, S., & Armelin, E. (2017). Poly(N-isopropylacrylamide) and copolymers: A review on recent progresses in biomedical applications. In *Gels* (Vol. 3, Issue 4). MDPI AG. https://doi.org/10.3390/gels3040036

Leszczynski, J., Koleżyński, A., & Król, M. (n.d.). *Challenges and Advances in Computational Chemistry and Physics Series Editor: Molecular Spectroscopy-Experiment and Theory From Molecules to Functional Materials*. http://www.springer.com/series/6918

Lewars, E. G. (2011). Computational chemistry: Introduction to the theory and applications of molecular and quantum mechanics. In *Computational Chemistry: Introduction to the Theory and Applications of Molecular and Quantum Mechanics*. Springer Netherlands. https://doi.org/10.1007/978-90-481-3862-3

Longhi, G., Lebon, F., Abbate, S., & Fornili, S. L. (2004). Molecular dynamics simulation of a model oligomer for poly(N- isopropylamide) in water. *Chemical Physics Letters*, *386*(1–3), 123–127. https://doi.org/10.1016/j.cplett.2004.01.045

Ortiz De Solorzano, I., Bejagam, K. K., An, Y., Singh, S. K., & Deshmukh, S. A. (2020). Solvation dynamics of: N -substituted acrylamide polymers and the importance for phase transition behavior. *Soft Matter*, *16*(6), 1582–1593. https://doi.org/10.1039/c9sm01798d

Pang, J., Yang, H., Ma, J., & Cheng, R. (2011). Understanding different LCST levels of poly(N-alkylacrylamide)S by molecular dynamics simulations and quantum mechanics calculations. *Journal of Theoretical and Computational Chemistry*, *10*(3), 359–370. https://doi.org/10.1142/S0219633611006505

PyMOL | *pymol.org*. (n.d.). Retrieved December 13, 2022, from https://pymol.org/2/

Qiu, Y., & Park, K. (2001). Environment-sensitive hydrogels for drug delivery. In *Advanced Drug Delivery Reviews* (Vol. 53). www.elsevier.com/locate/drugdeliv

Roth, P. J., Collin, M., & Boyer, C. (2013). Advancing the boundary of insolubility of non-linear PEG-analogues in alcohols: UCST transitions in ethanol-water mixtures. *Soft Matter*, *9*(6), 1825–1834. https://doi.org/10.1039/c2sm27427b

Roy, D., Brooks, W. L. A., & Sumerlin, B. S. (2013a). New directions in thermoresponsive polymers. *Chemical Society Reviews*, *42*(17), 7214–7243. https://doi.org/10.1039/c3cs35499g

Schattling, P., Jochum, F., Chemistry, P. T.-P., & 2014, undefined. (n.d.). Multi-stimuli responsive polymers–the all-in-one talents. *Pubs.Rsc.Org*. Retrieved August 2, 2022, from https://pubs.rsc.org/en/content/articlehtml/2014/py/c3py00880k

Sherrill, C. D. (2017). *Distinguishing Basis Set Superposition Error (BSSE) from Basis Set Incompleteness Error (BSIE)*.

Suwa, K., Morishita, K., Kishida, A., & Akashi, M. (1997). Synthesis and Functionalities of Poly(N-Vinylalkylamide). V. Control of a Lower Critical Solution Temperature of Poly (N-Vinylalkylamide). In *J Polym Sci A: Polym Chem* (Vol. 35). John Wiley & Sons, Inc.

Taylor, L. D., & Cerankowski, L. D. (1975). Preparation of films exhibiting a balanced temperature dependence to permeation by aqueous solutions—a study of lower consolute behavior. *Journal of Polymer Science: Polymer Chemistry Edition*, *13*(11), 2551–2570. https://doi.org/10.1002/POL.1975.170131113

Teotia, A. K., Sami, H., & Kumar, A. (2015). Thermo-responsive polymers: structure and design of smart materials. *Switchable and Responsive Surfaces and Materials for Biomedical Applications*, 3–43. https://doi.org/10.1016/B978-0-85709-713-2.00001-8

Teraoka, Iwao. (2002). *Polymer solutions : an introduction to physical properties*. Wiley.

Ward, M., Polymers, T. G.-, & 2011, undefined. (2011). Thermoresponsive polymers for biomedical applications. *Mdpi.Com*, *3*, 1215–1242. https://doi.org/10.3390/polym3031215

Young, D. C. (2001). *Computational chemistry : a practical guide for applying techniques to real world problems*. Wiley.

Zhelavskyi, O. S., & Kyrychenko, A. (2019). Atomistic molecular dynamics simulations of the LCST conformational transition in poly(N-vinylcaprolactam) in water. *Journal of Molecular Graphics and Modelling*, *90*, 51–58. https://doi.org/10.1016/j.jmgm.2019.04.004

CURRICULUM VITAE

Name Surname **:Fatma Can KÜTÜK**

EDUCATION **:**

- **B.Sc.** **:** 2013, Gazi University, Faculty of Engineering, Department of Chemical Engineering

PROFESSIONAL EXPERIENCE AND REWARDS:

- 2020-2021 Inovamind, Project Engineer
- 2018-2020 Greiner Packaging, R&D and Project Engineer
- 2017-2018 Biofarma, Quality Control Analyst